



**Calhoun: The NPS Institutional Archive**

---

Theses and Dissertations

Thesis Collection

---

1983

Amplitude shading and phase weighting of a vertical linear array in the SOFAR channel by the linear minimum variance estimation technique.

McVicar, Daniel P.

Monterey, California. Naval Postgraduate School

---



Calhoun is a project of the Dudley Knox Library at NPS, furthering the precepts and goals of open government and government transparency. All information contained herein has been approved for release by the NPS Public Affairs Officer.

**Dudley Knox Library / Naval Postgraduate School**  
**411 Dyer Road / 1 University Circle**  
**Monterey, California USA 93943**

<http://www.nps.edu/library>













# NAVAL POSTGRADUATE SCHOOL

## Monterey, California



# THESIS

AMPLITUDE SHADING AND PHASE WEIGHTING OF A  
VERTICAL LINEAR ARRAY IN THE SOFAR CHANNEL  
BY THE LINEAR MINIMUM VARIANCE  
ESTIMATION TECHNIQUE

by

Daniel Patrick McVicar

December 1983

Thesis Advisor:

P. H. Moose

Approved for public release; distribution unlimited

T215648





REPORT DOCUMENTATION PAGE		READ INSTRUCTIONS BEFORE COMPLETING FORM	
1. REPORT NUMBER	2. GOVT ACCESSION NO.	3. RECIPIENT'S CATALOG NUMBER	
4. TITLE (and Subtitle) Amplitude Shading and Phase Weighting of a Vertical Linear Array in the SOFAR Channel by the Linear Minimum Variance Estimation Technique		5. TYPE OF REPORT & PERIOD COVERED Master's Thesis December 1983	
		6. PERFORMING ORG. REPORT NUMBER	
7. AUTHOR(s) Daniel Patrick McVicar		8. CONTRACT OR GRANT NUMBER(s)	
9. PERFORMING ORGANIZATION NAME AND ADDRESS Naval Postgraduate School Monterey, California 93943		10. PROGRAM ELEMENT, PROJECT, TASK AREA & WORK UNIT NUMBERS	
11. CONTROLLING OFFICE NAME AND ADDRESS Naval Postgraduate School Monterey, California 93943		12. REPORT DATE December 1983	
		13. NUMBER OF PAGES 90	
14. MONITORING AGENCY NAME & ADDRESS (if different from Controlling Office)		15. SECURITY CLASS. (of this report)	
		15a. DECLASSIFICATION/DOWNGRADING SCHEDULE	
16. DISTRIBUTION STATEMENT (of this Report) Approved for public release; distribution unlimited			
17. DISTRIBUTION STATEMENT (of the abstract entered in Block 20, if different from Report)			
18. SUPPLEMENTARY NOTES			
19. KEY WORDS (Continue on reverse side if necessary and identify by block number) Linear Minimum Variance Estimation Depth Estimation Vertical Linear Array SOFAR Channel			
20. ABSTRACT (Continue on reverse side if necessary and identify by block number) A single linear vertical passive array is used in the 'SOFAR' channel to determine the depth of a single underwater source at a constant range. The phase and amplitude weights applied to the array are determined by the linear minimum variance estimation technique. The resulting beam pattern is compared to the conventional time domain beamformer. It was found that the linear minimum variance estimation technique of amplitude shading and phase weighting was significantly superior to the conventional beamformer.			



Approved for public release; distribution unlimited.

Amplitude Shading and Phase Weighting of a Vertical Linear Array  
in the SOFAR Channel  
by the Linear Minimum Variance Estimation Technique

by

Daniel P. McVicar  
Captain, Canadian Armed Forces  
B. Eng., Nova Scotia Technical College, 1976

Submitted in partial fulfillment of the  
requirements for the degrees of

MASTER OF SCIENCE IN ENGINEERING ACOUSTICS

and

MASTER OF SCIENCE IN ELECTRICAL ENGINEERING

from the

NAVAL POSTGRADUATE SCHOOL  
December 1983



### ABSTRACT

A single linear vertical passive array is used in the 'SOFAR' channel to determine the depth of a single underwater source at a constant range. The phase and amplitude weights applied to the array are determined by the linear minimum variance estimation technique. The resulting beam pattern is compared to the conventional time domain beamformer. It was found that the linear minimum variance estimation technique of amplitude shading and phase weighting was significantly superior to the conventional beamformer.



## TABLE OF CONTENTS

I.	INTRODUCTION . . . . .	9
II.	GENERAL THEORY . . . . .	13
	A. RAY ACOUSTICS . . . . .	13
	B. ARRAY MODEL . . . . .	18
	C. LINEAR MINIMUM VARIANCE METHOD . . . . .	23
III.	EXPERIMENTAL PROCEDURE . . . . .	32
	A. BASIC ASSUMPTIONS . . . . .	32
	B. ' <u>A</u> ' MATRIX CALCULATION . . . . .	32
	C. ' <u>Z</u> ' MATRIX . . . . .	34
	D. RESULTING BEAM PATTERN . . . . .	34
	1. Using the Linear Minimum Variance Method . . . . .	34
	2. Using Linear Phase Shifts . . . . .	35
IV.	RESULTS . . . . .	40
	A. EXACT SOLUTION . . . . .	40
	B. FOUR DEPTHS WITH TWO RECEIVERS . . . . .	40
	C. TWENTY DEPTHS WITH TWO RECEIVERS . . . . .	40
	D. TWENTY DEPTHS WITH FIVE RECEIVERS . . . . .	41
	E. CONVENTIONAL BEAMFORMER . . . . .	41
	F. RANGE OF 250 KILOMETERS . . . . .	42
V.	DISCUSSION OF RESULTS AND RECOMMENDATIONS . . . . .	66
	APPENDIX A: RELATIVE TRAVEL TIME CALCULATION . . . . .	68
	APPENDIX E: INTERPOLATION OF RELATIVE TRAVEL TIME CALCULATIONS . . . . .	81





APPENDIX C: RESULTING BEAM PATTERN FOR CALCULATED  
WEIGHTS . . . . . 84  
LIST OF REFERENCES . . . . . 89  
INITIAL DISTRIBUTION LIST . . . . . 90



LIST OF TABLES

I. Relative Travel Times For 380 Meter Source  
Depth . . . . . 36

II. Slower Ray Travel Times For 250 km Range and  
380 m Source . . . . . 43

III. Faster Travel Times For 250 km Range and 380 m  
Source . . . . . 43



## LIST OF FIGURES

2.1	Circular Ray Path . . . . .	15
2.2	Single Ray Path Plot In Triangular SOFAR Channel . . . . .	29
2.3	Ray Plot For Assumed Sound Channel . . . . .	30
2.4	Array Model . . . . .	31
3.1	Relative Travel Time vs. Depth (220 meter source) . . . . .	37
3.2	Relative Travel Time vs. Depth (380 meter source) . . . . .	38
3.3	Straight Line Approx. of Rel. Trav. Time vs. Depth (source at 380 m) . . . . .	39
4.1	Beam Amplitude vs. Source Depth (5 depths 5 receivers) . . . . .	44
4.2	Beam Pattern (4 depths 2 receivers, source at 220 m) . . . . .	45
4.3	Beam Pattern (4 depths 2 receivers, source at 280 m) . . . . .	46
4.4	Beam Pattern (20 depths 2 receivers, source at 220 m) . . . . .	47
4.5	Beam Pattern (20 depths 2 receivers, source at 380 m) . . . . .	48
4.6	Beam Pattern (20 depths 5 receivers, source at 220 m) . . . . .	49
4.7	Beam Pattern (20 depths 5 receivers, source at 360 m) . . . . .	50
4.8	Beam Pattern (20 depths 5 receivers, source at 380 m) . . . . .	51
4.9	Beam Pattern (20 depths 5 receivers, source at 400 m) . . . . .	52



4.10	Conventional Beam Pattern (source at 380 meters) . . . . .	53
4.11	Conventional Beam Pattern (non-unity amp. wts. source at 380 m) . . . . .	54
4.12	Relative Travel Time vs. Depth (range=250 km, source at 220 m) . . . . .	55
4.13	Relative Travel Time vs. Depth (range=250 km, source at 380 m) . . . . .	56
4.14	St. Line Approx. of Rel. Trav. Time vs. Depth (R=250 km, d=380 m) . . . . .	57
4.15	Conventional Beam Pattern (R=250 km, d=380 m, slower times, a=1) . . . . .	58
4.16	Conventional Beam Pattern (R=250 km, d=380 m, slower times, LMV a) . . . . .	59
4.17	Conventional Beam Pattern (R=250 km, d=380 m, faster times, a=1) . . . . .	60
4.18	Conventional Beam Pattern (R=250 km, d=380 m, faster times, LMV a) . . . . .	61
4.19	Beam Pattern (R=250 km, 20 depths, 5 receivers, source at 220 m) . . . . .	62
4.20	Beam Pattern (R=250 km, 20 depths, 5 receivers, source at 340 m) . . . . .	63
4.21	Beam Pattern (R=250 km, 20 depths, 5 receivers, source at 360 m) . . . . .	64
4.22	Beam Pattern (R=250 km, 20 depths, 5 receivers, source at 380 m) . . . . .	65





## I. INTRODUCTION

There are many solutions to the problem of predicting the location of an underwater energy source. One common solution is the use of a passive hydrophone which detects the pressure waves radiating from the source. The hydrophone sensor is assumed to be omnidirectional and therefore incapable of estimating direction. To provide directionality a series of sensors are placed in a row to form a passive linear array.

A familiar method of determining directionality is time-domain beamforming. In this principle, it is assumed that the source is far enough away so that the pressure wave appears to be a plane wave when viewed at the site of the receiving array.

Thus a set of time delays are calculated for any direction of signal arrival, which, when applied to the receiver outputs causes them to be in phase and to reinforce when summed. The resultant angular response to signals arriving from other than the nominated direction is then a function of the array geometry, relative to the signal wavelength, and any weighting factors which have been applied to the receiver outputs. The effect is to generate a main receiving beam in the desired direction, with a series of undesired subsidiary sidelobes whose magnitude can be controlled to some extent by the choice of a suitable array geometry and the use of amplitude weightings on the receiver outputs.

In order to determine location, three or more such arrays separated by a known amount may be used.

This study is concerned with a single linear vertical passive array and the determination of the depth of a single



underwater source. The analysis is based on the following assumptions:

- The underwater source is emitting continuously and at a monochromatic frequency.
- Both the source and receiving hydrophones are stationary in space causing a constant range.
- The range is sufficiently long so that the channel is filled with R-R (refracted-refracted) rays.
- There is no distortion introduced in the propagating medium so that the signals received at each sensor are identical except for constant delays.
- The source signal and noise are independent and stationary gaussian random processes.
- The speed of sound profile is triangular and symmetric with the deep sound channel axis at 1000 meters. The velocity gradient is  $-0.017$  meters/meter/sec above 1000 meters and  $+0.017$  meters/meter/sec below 1000 meters. This profile gives a speed of sound at the surface of 1500 meters/sec.
- The speed of sound profile is constant in the horizontal plane.
- Only R-R rays are considered. All other rays have sufficient loss that their effect is negligible.

As opposed to conventional time-domain beamforming, this study makes no assumption of planar wave fronts at the receiver site. Therefore the time delays applied to each receiver will not, in general, be a linear function of depth.

Since it is desired to determine whether or not there is a source present at a specific depth the result will be a



binary decision. A "1" will indicate signal source present; a "0" will indicate signal source not present. For the constant range there will be "N" test depths investigated for the signal source. The number of hydrophones in the vertical array will be "L".

For a single source at a given depth, the travel time is calculated from the depth to each hydrophone. This travel time is converted into a phase delay for each hydrophone so that after summation from all hydrophones a maximum output is achieved. This output is then passed through a squaring device, an integrator, and a threshold and flip flop device to give a "1" binary output. If the signal source is at a different depth and the same previous phase delays are used for each hydrophone then the output will be somewhat less than the previous maximum. The difference in depth required to achieve a "0" binary output is the depth resolution of the system.

The travel times for each hydrophone are calculated for each of the "N" source depths to be considered. "N" will ordinarily be much greater than "L" so that the system will be overdetermined. An overdetermined system is one in which there are more equations than unknowns. The objective then is to calculate the phase angle and amplitude weight for each hydrophone so that a determination can be made indicating the presence or absence of a signal source at a given depth.

The method used to calculate the phase and amplitude weights is the linear minimum variance estimation technique. Linear minimum variance estimators are optimum when compared with all other estimators for gaussian problems. The method is directly applicable to overdetermined systems.

The output of the summer is calculated using the linear minimum variance amplitude and phase angles assuming a source at one of the "N" source depths and no source at the



others. The calculation is repeated for each of the depths. The result, when plotted against source depth, will be referred to as the "beam pattern" of the array in this report. (Although similar, it should not be interpreted as the angular response of an array as in the conventional definition of a beam pattern. The conventional definition loses much of its utility when the wavefronts are not planar.) Ideally the beam pattern will be maximum at the desired depth and very small at all other depths so that the binary "1" decision will be made for a source at the desired depth, and a "0" decision for sources at all others. This beam pattern is compared with the depth beam pattern of the conventional time-domain beamformer mentioned above. The purpose of this thesis is to determine, as an initial investigation, whether the linear minimum variance estimation technique, when applied to a linear vertical array, is useful in depth discrimination at long ranges in a 'SOFAR' type sound channel.





## II. GENERAL THEORY

### A. RAY ACOUSTICS

The propagation of sound in an elastic medium can be described mathematically by solutions of the wave equation using the appropriate boundary and medium conditions for a particular problem. The wave equation relating the acoustic pressure 'p' to the coordinates 'x', 'y', 'z', and the time 't', may be written as

$$\frac{d^2 p}{dt^2} = c^2 \left( \frac{d^2 p}{dx^2} + \frac{d^2 p}{dy^2} + \frac{d^2 p}{dz^2} \right) \quad (2.1)$$

where 'c' is a quantity that has the general significance of sound velocity and may vary with the coordinates.

One may approximate the solution of the wave equation using ray theory: its body of results and conclusions is called ray acoustics.

Officer [Ref. 1] describes the ray solution as a complete solution to any particular propagation problem within the validity of the approximation of the Eikonal equation to the wave equation. For these approximations to be valid neither the amplitude of the wave nor the speed of sound can change appreciably in distances comparable to a wavelength.

Thus the path of a ray through a medium in which the speed of sound varies with depth can be calculated by the application of Snell's law

$$\cos\theta/c = 1/c_0 = \text{a constant for any one ray} \quad (2.2)$$



where 'e' is the angle of depression made with the horizontal at a depth where the speed of sound is 'c', and 'c<sub>0</sub>' is the speed at a depth (real or extrapolated) where the ray would become horizontal.

In a medium in which the velocity of sound changes linearly with depth the sound rays can be shown to be arcs of circles, that is, to have a constant radius of curvature. Kinsler et al. [Ref. 2] give a simple and heuristic demonstration of the circularity of rays in a medium with a linear sound speed gradient 'g'. The center of the circle which creates the arc lies at a depth where the sound speed extrapolates to zero. To understand this, consider a portion of a ray path with a local radius of curvature 'R', as illustrated in Figure 2.1. Since the gradient 'g' for this case is

$$g = \Delta c / \Delta z = (c_2 - c_1) / (d_2 - d_1) = (c_2 - c_1) / R (\cos \theta_1 - \cos \theta_2) \quad (2.3)$$

where ' $\Delta c$ ' is the change in sound speed and ' $\Delta z$ ' is the change in depth. It can be seen that the radius of curvature is given by

$$R = -c_0 / g = -c / (g \cos \theta) \quad (2.4)$$

The ray path is therefore a circle when 'g' is constant because 'R' is then constant. The center of curvature of a circle lies at the depth where  $\theta$  is 90 degrees, which corresponds to  $c=0$ . For the situation in Figure 2.1 the speed gradient is negative so that 'R' is positive. If the speed gradient were positive 'R' would be negative, and the path would curve upward.

Once the radius of curvature of each segment of a path is known the actual path can be traced graphically or



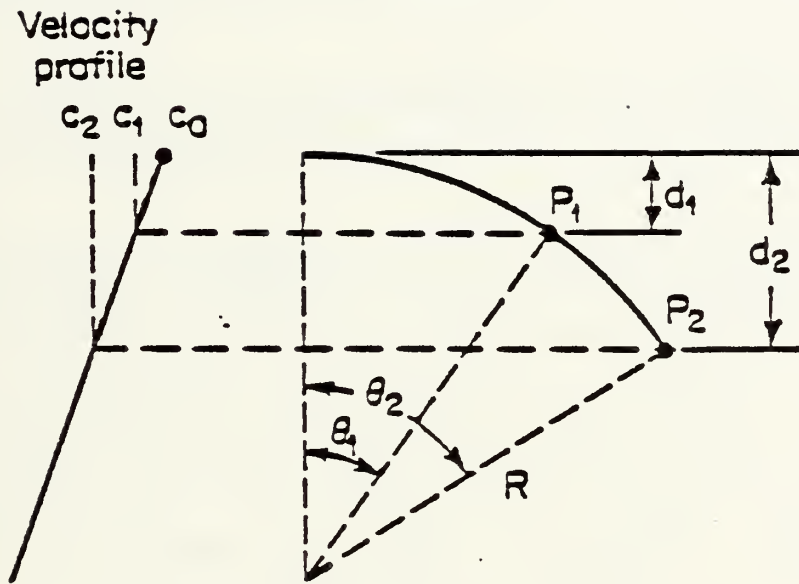


Figure 2.1 Circular Ray Path



computed. If the initial angle of depression of a ray is  $\theta_1$ , then by referring to the geometry of Figure 2.1 the changes in both range and depth are

$$\Delta r = c_1 (\sin(\theta_1) - \sin(\theta_2)) / (g \cos(\theta_1)) \quad (2.5)$$

$$\Delta z = c_1 (\cos(\theta_2) - \cos(\theta_1)) / (g \cos(\theta_1)) \quad (2.6)$$

The sign convention for these equations is: downward, to the right, and depression angles below the horizontal axis positive.

The symmetric triangular sound speed profile assumed in the introduction is similar to speed profiles encountered in the deep sound channel, sometimes called the SOFAR channel. The velocity minimum which occurs at the axis of the sound channel causes the sea to act like a kind of lens; above and below the minimum, the velocity gradient continually bends the sound rays toward the depth of minimum velocity. A portion of the power radiated by a source in the deep sound channel accordingly remains within the channel and encounters no acoustic losses by reflection from the surface and bottom. These rays are called R-R (refracted-refracted) and since they have very low transmission loss, very long ranges can be obtained from a source of moderate acoustic power output. Thus an energy source at a specific depth will propagate energy in all directions but only the direction which is toward the receiving array and for which the rays are R-R is of interest. To determine the range of depression angles which will yield R-R rays Snell's law is used to give





$$\theta_{\max} = \arccos(c_1 / (c_1 - g d)) \quad (2.7)$$

where ' $\theta_{\max}$ ' is in radians and ' $c_1$ ' is the speed of sound at the source depth ' $d$ '.

An example is given in Figure 2.2 of a single ray trace propagating in the SOFAR channel to show how equations 2.5 and 2.6 are used in determining range and depth. The ray path is broken up into arcs of circles as shown in the figure, and then by paying close attention to the previously defined sign conventions, the change in range and depth is found. Being more specific, for arc 1,  $\theta_1$  and  $\theta_2$  are both positive; for arc 2,  $\theta_1$  is positive and  $\theta_2$  is zero; for arc 3,  $\theta_1$  is zero and  $\theta_2$  is negative; and for arc 4,  $\theta_1$  is negative and  $\theta_2$  is zero. By keeping a running total of all the depth and range changes it is possible to determine the total horizontal distance travelled and the depth at that distance.

For the speed of sound profile assumed in the introduction a computer generated ray plot is shown in Figure 2.3 for a source depth of 300 meters. As each ray propagates out from the source the triangular channel becomes filled with sound. If a receiving hydrophone is placed a great distance away, a number of refracted propagation paths will exist, each having a different travel time and crossing the channel axis at different intervals. The path with the greatest excursion from the axis will have the shortest travel time.

Officer [Ref. 1] shows that the travel time ' $t$ ' of a ray, which is an arc of a circle, is given by

$$t = \frac{1}{g} \int_{\theta_1}^{\theta_2} \frac{d\theta}{\cos\theta} \quad (2.8)$$

and the travel time for each arc is



$$t = -\frac{1}{g} \log_e \left[ \frac{\tan((\pi/4) + (\theta_2/2))}{\tan((\pi/4) + (\theta_1/2))} \right] \quad (2.9)$$

Equation 2.9, applied using the same convention as equations 2.5 and 2.6, determines the total travel time of a ray in the deep sound channel.

## B. ARRAY MODEL

The receiving linear vertical array is presumed to consist of 'L' hydrophones as shown in Figure 2.4. It is assumed that the source is emitting energy at a constant frequency, 'f', and amplitude, 'A', regardless of the depth. The source signal at the source is  $A \exp(j2\pi ft)$ . The inherent received signal at the first hydrophone is

$$x_1(t) = A \exp(j2\pi f(t-t_1)) \quad (2.10)$$

where 't<sub>1</sub>' is the travel time from the energy source to the first hydrophone and 'A' is the amplitude of the signal at the range of the array. After passage through the amplitude weight 'a<sub>1</sub>' and a phase delay of 'τ<sub>1</sub>', the signal on the first hydrophone at the input to the summer is

$$y_1(t) = A' a_1 x_1(t - \tau_1) = A' a_1 \exp(j2\pi f(t - t_1 - \tau_1)) \quad (2.11)$$

A time delay, for monochromatic signals corresponds to a phase shift

$$\theta = 2\pi ft \quad (2.12)$$

where 'θ' is the phase shift in radians and 't' is the time delay in seconds. Thus equation 2.11 can be written as



$$y_1(t) = A' a_1 \exp(j(2\pi ft - \phi_1 - \theta_1)) \quad (2.13)$$

where ' $\phi_1 = 2\pi ft_1$ ' is the phase delay due to the travel time from the source to the first hydrophone and ' $\theta_1$ ' is the phase delay in the receiver on the first hydrophone.

Combining all the hydrophones in the array in a summer gives as an expression for the array output

$$Y(t) = \sum_{k=1}^L A' a_k \exp(j(2\pi ft - \phi_k - \theta_k)) \quad (2.14)$$

where ' $\phi_k$ ' represents the phase delay due to the travel time from the source to the "k th" hydrophone and ' $\theta_k$ ' is the phase delay in the receiver on the "k th" hydrophone. If the amplitude of the energy source is normalized by setting  $A'=1$ , and equation 2.14 is written in terms of real and imaginary components, we have

$$Y(t) = \sum_{k=1}^L a_k \cos(-\phi_k - \theta_k) + j \sin(-\phi_k - \theta_k) \exp(j2\pi ft) \quad (2.15)$$

When an energy source is at the "q th" depth, we wish to have each receiving hydrophone's phase delay cancel out the effect of the travel time from the source to it, such that ' $-\phi_k - \theta_k$ ' is equal to a multiple of ' $2\pi$ '. This will put all signals into the summer in phase and thus maximize the signal gain for a source at the "q th" depth. From equation 2.15,

$$\sum_{k=1}^L (a_{kq} \cos(-\phi_{kq} - \theta_{kq})) = L \quad (\text{source present at } q) \quad (2.16)$$

$$\sum_{k=1}^L (a_{kq} \sin(-\phi_{kq} - \theta_{kq})) = 0 \quad (\text{source present at } q) \quad (2.17)$$



Note that the first subscript on the phase angle indicates the receiving hydrophone and the second subscript indicates the depth of the source. Thus ' $\phi_{kq}$ ' would indicate the phase shift relating to the travel time from the "q th" test depth to the "k th" hydrophone in the receiving array.

It is desirable for ' $Y(t)$ ' to be a minimum value for sources at other than the depth being investigated. Thus for each of the other ' $N-1$ ' depths ' $Y(t)$ ' is set to zero. This gives ' $N-1$ ' equations for the real terms of ' $Y(t)$ ' set to zero

$$\sum_{k=1}^L a_{kq} \cos(-\phi_{km} - \theta_{kq}) = 0 \quad (\text{source absent; } m \neq q) \quad (2.18)$$

and ' $N-1$ ' equations for the imaginary terms of ' $Y(t)$ ' set to zero

$$\sum_{k=1}^L a_{kq} \sin(-\phi_{km} - \theta_{kq}) = 0 \quad (\text{source absent; } m \neq q) \quad (2.19)$$

By using elementary trigonometric identities, equation 2.16 (real terms with source present at "q th" depth) becomes

$$\sum_{k=1}^L a_{kq} [\cos(\phi_{kq}) \cos(\theta_{kq}) - \sin(\phi_{kq}) \sin(\theta_{kq})] = L \quad (2.20)$$

Equation 2.18 (real terms with source absent for each of the other ' $N-1$ ' depths) becomes

$$\sum_{k=1}^L a_{kq} [\cos(\phi_{km}) \cos(\theta_{kq}) - \sin(\phi_{km}) \sin(\theta_{kq})] = 0 \quad m=1,2,\dots,N; m \neq q \quad (2.21)$$

Equation 2.17 (imaginary terms with source present at the "q th" depth) becomes





$$\sum_{k=1}^L -a_{kq} (\sin(\phi_{kq}) \cos(\theta_{kq}) + \cos(\phi_{kq}) \sin(\theta_{kq})) = 0 \quad (2.22)$$

and equation 2.19 (imaginary terms with source absent for each of the other 'N-1' depths) becomes

$$\sum_{k=1}^L -a_{kq} [\sin(\phi_{km}) \cos(\theta_{kq}) + \cos(\phi_{km}) \sin(\theta_{kq})] = 0 \quad m=1,2,\dots,N; m \neq q \quad (2.23)$$

Thus, there are a total of '2N' equations with '2L' unknowns.

In order to simplify, we put these '2N' equations into matrix form. Arbitrarily the real terms are made the first 'N' equations and the imaginary terms the second 'N' equations. The first real and first imaginary equation is at the lowest (shallowest) source depth and equations increase in order after that until the last real and last imaginary equation correspond to a source at the deepest depth. The resultant matrix equation becomes:

$$\begin{bmatrix} 0 \\ 0 \\ \cdot \\ \cdot \\ 0 \\ L \\ 0 \\ \cdot \\ \cdot \\ 0 \\ 0 \\ \cdot \\ \cdot \\ 0 \\ 0 \\ \cdot \\ \cdot \\ 0 \end{bmatrix} = \begin{bmatrix} \cos\phi_{11} & \cos\phi_{21} & \dots & \cos\phi_{L1} & -\sin\phi_{11} & -\sin\phi_{21} & \dots & -\sin\phi_{L1} \\ \cos\phi_{12} & \cos\phi_{22} & \dots & \cos\phi_{L2} & -\sin\phi_{12} & -\sin\phi_{22} & \dots & -\sin\phi_{L2} \\ \cdot & \cdot & & \cdot & \cdot & \cdot & & \cdot \\ \cdot & \cdot & & \cdot & \cdot & \cdot & & \cdot \\ 0 & & & & & & & \\ L & \cos\phi_{1q} & \cos\phi_{2q} & \dots & \cos\phi_{Lq} & -\sin\phi_{1q} & -\sin\phi_{2q} & \dots & -\sin\phi_{Lq} \\ 0 & \cdot & \cdot & & \cdot & \cdot & & \cdot \\ \cdot & \cdot & \cdot & & \cdot & \cdot & & \cdot \\ 0 & \cos\phi_{1N} & \cos\phi_{2N} & \dots & \cos\phi_{LN} & -\sin\phi_{1N} & -\sin\phi_{2N} & \dots & -\sin\phi_{LN} \\ 0 & -\sin\phi_{11} & -\sin\phi_{21} & \dots & -\sin\phi_{L1} & -\cos\phi_{11} & -\cos\phi_{21} & \dots & -\cos\phi_{L1} \\ 0 & -\sin\phi_{12} & -\sin\phi_{22} & \dots & -\sin\phi_{L2} & -\cos\phi_{12} & -\cos\phi_{22} & \dots & -\cos\phi_{L2} \\ \cdot & \cdot & \cdot & & \cdot & \cdot & & \cdot \\ \cdot & \cdot & \cdot & & \cdot & \cdot & & \cdot \\ 0 & -\sin\phi_{1N} & -\sin\phi_{2N} & \dots & -\sin\phi_{LN} & -\cos\phi_{1N} & -\cos\phi_{2N} & \dots & -\cos\phi_{LN} \end{bmatrix} \begin{bmatrix} a_{1q} \cos\theta_{1q} \\ a_{2q} \cos\theta_{2q} \\ \cdot \\ \cdot \\ \cdot \\ \cdot \\ a_{Lq} \cos\theta_{Lq} \\ a_{1q} \sin\theta_{1q} \\ a_{2q} \sin\theta_{2q} \\ \cdot \\ \cdot \\ \cdot \\ a_{Lq} \sin\theta_{Lq} \end{bmatrix} \quad (2.24)$$

Simplifying further, equation 2.24 becomes:







Equation 2.27 represents '2N' equations. Since this system of equations is overdetermined ( $N > L$ ) an exact solution does not exist. In order to make the best estimate of  $\underline{\theta}$  for the desired response, the linear minimum variance estimation technique is used.

### C. LINEAR MINIMUM VARIANCE METHOD

Equation 2.27 represents a noise free environment. If noise were present it would become

$$\underline{Z} = \underline{A}\underline{\theta} + \underline{n} \quad (2.28)$$

with ' $\underline{n}$ ' a "2N" element column vector. This represents the noise at each source depth. ' $\underline{Z}$ ' is a linear function of ' $\underline{\theta}$ ' and is called the observation. ' $\underline{A}$ ' is a "2Nx2L" modulation or observation matrix which is known, and ' $\underline{\theta}$ ' is the "2L" element random parameter vector which is to be estimated. Assume the first and second moments of ' $\underline{\theta}$ ' and ' $\underline{n}$ ' are given by

$$E(\underline{\theta}) = \underline{\mu}_{\theta} \quad \text{Var}(\underline{\theta}) = \underline{V}_{\theta} \quad (2.29)$$

and

$$E(\underline{n}) = \underline{0} \quad \text{Var}(\underline{n}) = \underline{V}_n \quad (2.30)$$

where 'E' represents expectation or first moment and 'Var' represents the covariance matrix. It is assumed that the parameter ' $\underline{\theta}$ ' and the noise ' $\underline{n}$ ' are uncorrelated.

A restriction imposed is that the estimate must be a weighted linear combination of the observations:



$$\hat{\underline{\theta}}_L = \underline{b} + \underline{E}\underline{Z} \quad (2.31)$$

where '^' indicates estimate. The objective is to select 'b' and 'B' in order to minimize the error variance. Such an estimator is the linear minimum variance estimator; it is the best, in the sense of minimum-error-variance linear estimators.

Another restriction is that the estimator be unbiased; in other words it is required that the expected value of the estimator ' $\hat{\underline{\theta}}_L$ ' is equal to the expected value of the parameter ' $\underline{\theta}$ '. Thus,

$$E(\hat{\underline{\theta}}_L) = \underline{b} + \underline{B}E(\underline{z}) = E(\underline{\theta}) = \underline{\mu}_\theta \quad (2.32)$$

yielding

$$\underline{b} = \underline{\mu}_\theta - \underline{B}\underline{A}\underline{\mu}_\theta \quad (2.33)$$

Substituting this result in equation 2.31 gives for the unbiased linear estimator

$$\hat{\underline{\theta}}_L = \underline{\mu}_\theta + \underline{B}(\underline{Z} - \underline{A}\underline{\mu}_\theta) \quad (2.34)$$

Note that since the estimator is unbiased, the estimation error ' $\underline{\theta}_E = \underline{\theta} - \hat{\underline{\theta}}_L$ ' is zero mean. The next step is to select 'B' in order to minimize the error variance. However, this optimization problem is ill-defined because the error variance is a matrix. Therefore in order to introduce a scalar goodness measure the sum of the variances of each component of ' $\underline{\theta}$ ' is minimized. This is the sum of the main diagonal terms of the covariance matrix and is defined as the trace of the matrix.





$$\text{tr} (\text{Var}(\underline{\theta}_E)) = \sum_{n=1}^{2N} \text{Var}((\underline{\theta}_E)_n) \quad (2.35)$$

where 'tr' indicates trace. 'B' is then selected to minimize the trace of the error variance, or

$$\min_B \text{tr} (\text{Var}(\underline{\theta}_E)) = \min_B \text{tr} (E(\underline{\theta}_E \underline{\theta}_E^T)) \quad (2.36)$$

where '<sup>T</sup>' indicates the transpose. The following problem is then obtained by substituting equation 2.34 into equation 2.36:

$$\min_B \text{tr} (\text{Var}(\underline{\theta}_E)) = \min_B \text{tr} (E((\underline{\theta} - \underline{u}_\theta - \underline{B}(\underline{Z} - \underline{A}\underline{u}_\theta))(\underline{\theta} - \underline{u}_\theta - \underline{B}(\underline{Z} - \underline{A}\underline{u}_\theta))^T)) \quad (2.37)$$

It is well known [Ref. 3] that equation 2.37 is minimized when

$$\text{Cov}(\underline{\theta}, \underline{Z}) - \underline{B} \text{Var}(\underline{Z}) = \underline{0} \quad (2.38)$$

where 'Cov(θ, Z)' is the covariance matrix of the unknown parameters and the observations. Denoting the optimum filter by 'B<sup>\*</sup>', then if

$$\underline{B}^* = \text{Cov}(\underline{\theta}, \underline{Z}) (\text{Var}(\underline{Z}))^{-1} \quad (2.39)$$

a minimum is achieved for the sum of the squares of the errors.

Using equation 2.28 for 'Z', the covariance of 'θ' and 'Z' becomes

$$\text{Cov}(\underline{\theta}, \underline{Z}) = \text{Cov}(\underline{\theta}, \underline{A}\underline{\theta} + \underline{n}) = \underline{V}_\theta \underline{A}^T \quad (2.40)$$

since 'θ' and 'n' are uncorrelated. The variance of 'Z' is



$$\text{Var}(\underline{Z}) = \text{Var}(\underline{A}\underline{\theta} + \underline{n}) = \underline{A}\underline{V}\underline{A}^T + \underline{V}_n \quad (2.41)$$

Substituting these into equation 2.39 gives

$$\underline{B}^* = \underline{V}_\theta \underline{A}^T (\underline{A}\underline{V}_\theta \underline{A}^T + \underline{V}_n)^{-1} \quad (2.42)$$

and the linear minimum variance estimator is

$$\hat{\underline{\theta}}_{\text{LMV}} = \underline{\mu}_\theta + \underline{V}_\theta \underline{A}^T (\underline{A}\underline{V}_\theta \underline{A}^T + \underline{V}_n)^{-1} (\underline{Z} - \underline{A}\underline{\mu}_\theta) \quad (2.43)$$

By utilizing a matrix inversion lemma [Ref. 3] equation 2.43 becomes

$$\hat{\underline{\theta}}_{\text{LMV}} = (\underline{A}^T \underline{V}_n^{-1} \underline{A} + \underline{V}_\theta^{-1})^{-1} (\underline{A}^T \underline{V}_n^{-1} \underline{Z} + \underline{V}_\theta^{-1} \underline{\mu}_\theta) \quad (2.44)$$

The advantage of this equation over equation 2.43 is the size of the matrix to be inverted. In equation 2.43 the matrix has dimensionality '2N' while in equation 2.44 its dimensionality is only '2L'. Thus the advantages of the linear variance estimator are the ease with which they are derived, the mathematical tractability of the linear form, and the minimum amount of stochastic information required for development. An interesting characteristic is that the linear minimum variance estimate is the orthogonal projection of 'θ' onto the space spanned by the observation 'Z'. Because of these factors this estimator is a popular form for estimating unknowns in overdetermined equations.

For this thesis it is assumed that the noise samples are uncorrelated and identically distributed so that:

$$\underline{V}_n = \sigma^2 \underline{I} \quad (2.45)$$



No previous knowledge is assumed about ' $\theta$ '. This implies an infinite variance matrix which is represented as:

$$\underline{v}_{\theta}^{-1} = \underline{0} \quad \text{and} \quad \underline{\mu}_{\theta} = \underline{0} \quad (2.46)$$

The linear minimum variance estimate given by equation 2.44 is then

$$\hat{\underline{\theta}}_{LMV} = (\underline{A}^T \underline{A})^{-1} \underline{A}^T \underline{Z} \quad (2.47)$$

By determining ' $\hat{\underline{\theta}}_{LMV}$ ', the phase and amplitude weights are found for a signal source on the ' $q$  th' depth. Recall that

$$\hat{\underline{\theta}}_{LMV} = \begin{bmatrix} \hat{\theta}_1 \\ \hat{\theta}_2 \\ \vdots \\ \hat{\theta}_L \\ \hat{\theta}_{L+1} \\ \vdots \\ \hat{\theta}_{2L} \end{bmatrix} = \begin{bmatrix} a_{1q} \cos \theta_{1q} \\ a_{2q} \cos \theta_{2q} \\ \vdots \\ a_{Lq} \cos \theta_{Lq} \\ a_{1q} \sin \theta_{1q} \\ \vdots \\ a_{Lq} \sin \theta_{Lq} \end{bmatrix} \quad (2.48)$$

Upon solving, this equation gives for the phase delay

$$\hat{\theta}_{mq} = \arctan(\hat{\theta}_{L+m} / \hat{\theta}_m) \quad \text{where } m=1 \text{ to } L \quad (2.49)$$

and amplitude weight

$$\hat{a}_{mq} = \hat{\theta}_m / \cos(\hat{\theta}_{mq}) \quad \text{where } m=1 \text{ to } L \quad (2.50)$$

When these amplitude weights and phase delays are applied to the vertical linear array a resulting beam pattern is formed which in the absence of noise is:



$$\hat{Z} = \hat{A}\hat{\theta}$$

(2.51)

The resulting beam pattern 'Z' can then be compared with the desired beam pattern 'Z', as well as with a conventional beam pattern 'Z' obtained using linear phase shifts across the array aperture selected to "steer" the array to the dominant arrival angle for the selected source depth.





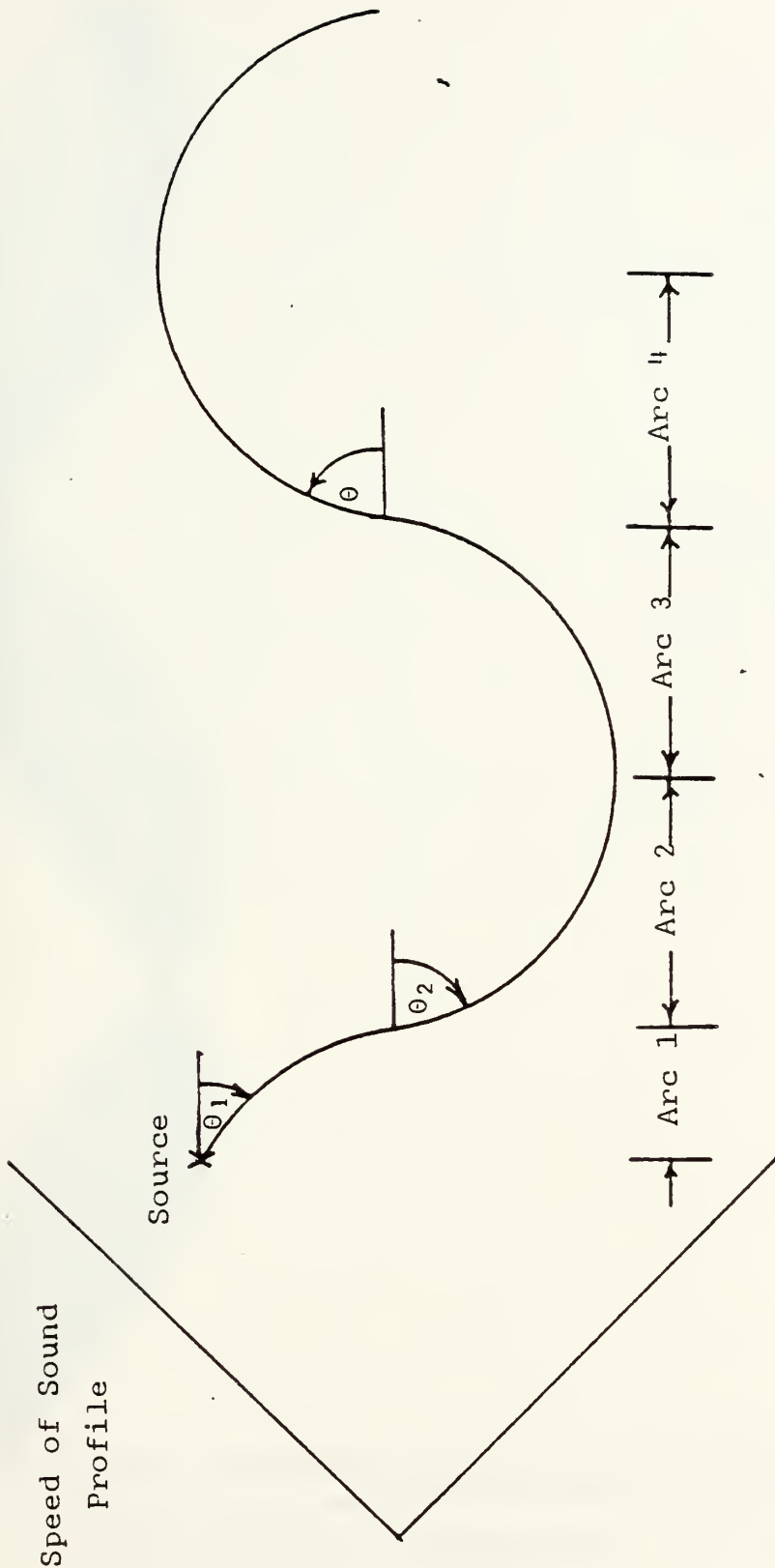


Figure 2.2 Single Ray Path Plot In Triangular SOFAR Channel



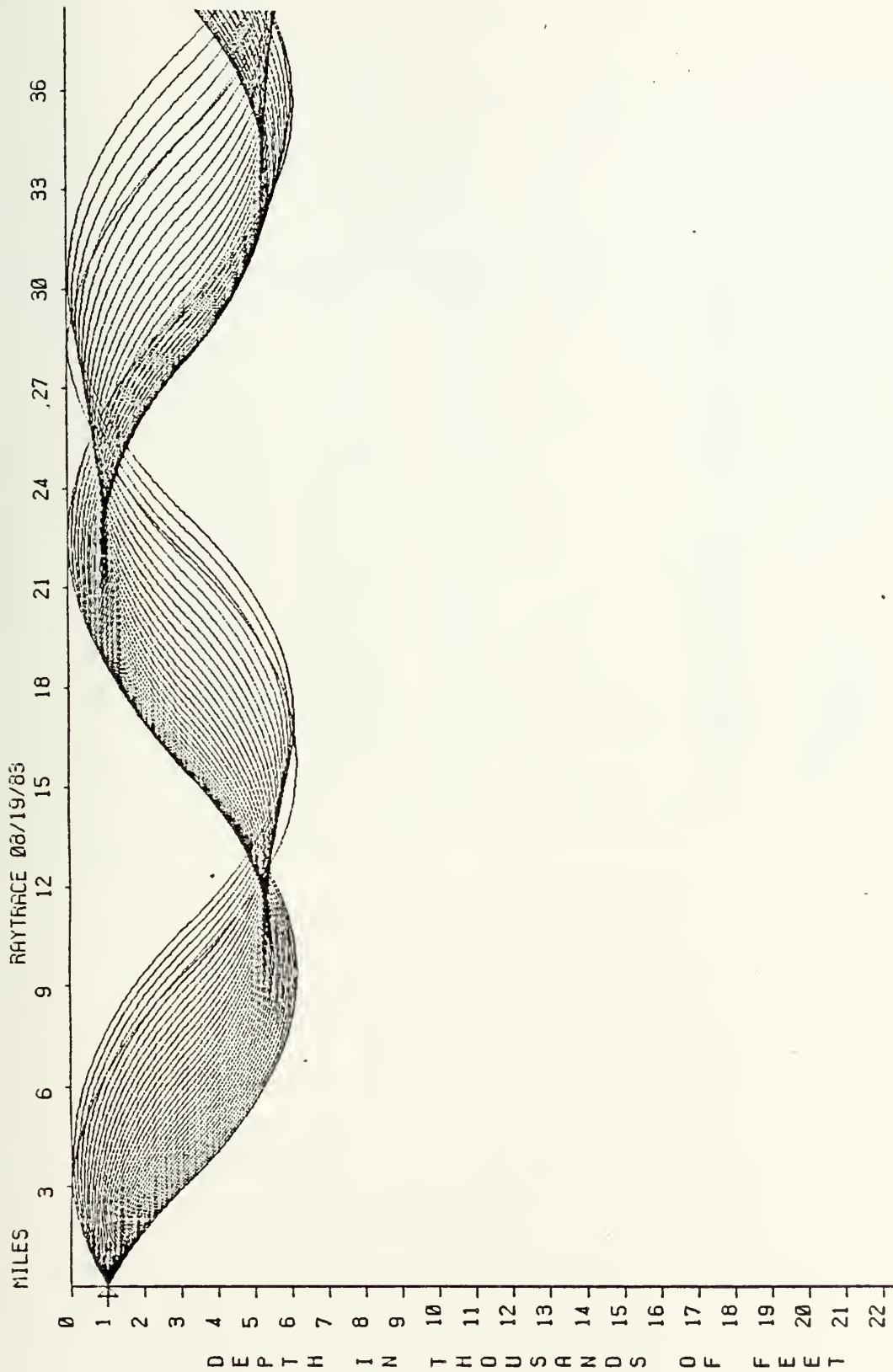
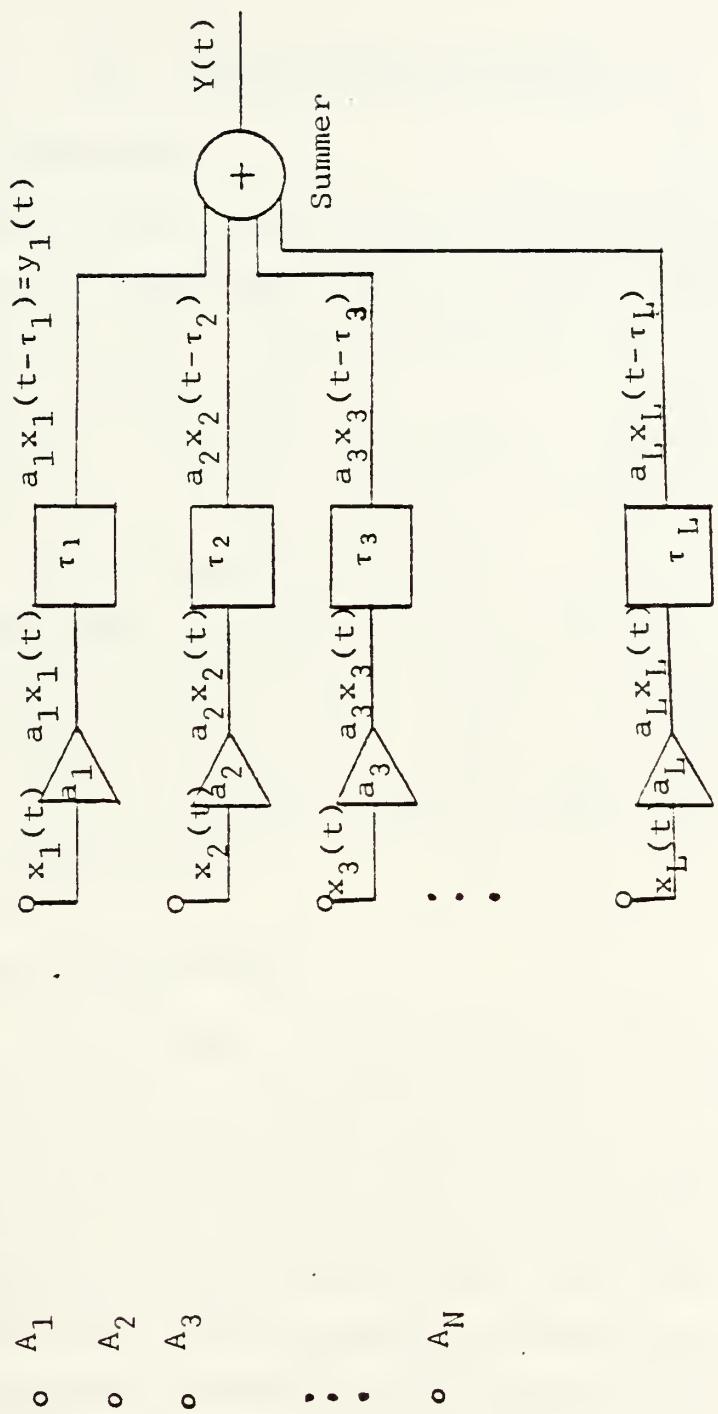


Figure 2.3 Ray Plot For Assumed Sound Channel



Vertical Linear Array

Source Depths



Amplitude Weights      Phase Delays

Figure 2.4 Array Model



### III. EXPERIMENTAL PROCEDURE

#### A. BASIC ASSUMPTIONS

The speed of sound profile given in the Introduction was used to test the technique, with 'L', the number of source depths chosen as 20. The source depths are at 220 meters and every 20 meters thereafter to 600 meters inclusive. 'N', the number of hydrophones used in the vertical array was chosen as 5. The hydrophones are placed at depths of 100, 200, 300, 400, and 500 meters. Thus, there are 40 equations, two for each source depth, and 10 unknowns, two for each hydrophone. A range of 200 kilometers (km) assures that the deep sound channel is filled with sound over the aperture of the vertical linear array. A frequency of 100 Hz provides good resolution in the beam pattern without introducing alias mainlobes at the selected range across the depths of investigation.

#### B. 'A' MATRIX CALCULATION

Since the gradient of the sound velocity, 'g' is constant in the area of the source depths, and the speed of sound at the surface is known, equation 2.3 is used to solve for 'c2', the speed of sound at the source depth. Equation 2.7 is used for each source depth to calculate the maximum initial depression angle which yields R-R rays. In determining travel time, only depression angles from each source which are positive (downward) and yield R-R rays are used.

Beginning with the first source depth of 220 meters, an initial depression angle of 0.0 degrees is selected. The ray path is then calculated using equations 2.5 and 2.6 and broken into a series of arcs as in figure 2.2. Equation 2.9





is used to determine the travel time for each arc in the same manner. Each arc's horizontal range, travel time, and depth are summed. When the summed horizontal range reaches 200 km the summation process ends. The travel time and depth of the ray at this horizontal range is then known. The same procedure is repeated for an initial depression angle of 0.1 degrees and every increment of 0.1 degrees thereafter until the maximum depression from equation 2.7 is reached. The final ray path is at this maximum depression angle.

The same procedure is repeated for each of the other 19 source depths.

Thus, for each initial angle from each source depth there is a ray which has a travel time and a depth when it reaches the horizontal range of 200 km. Since it is the profile of the sound pressure wave which impinges on the vertical array which is of importance, a constant can be subtracted from these calculated travel times. This constant is selected to be the travel time for the source depth of 220 meters which has an initial depression angle of 0 degrees. It is subtracted from each of the travel times making the resultant travel times relative with respect to the ray which has a 0 degree depression angle from the 220 meter depth. The program and its listing which calculates the relative travel times and the depths of these rays at the horizontal range of 200 km is given in Appendix A.

A plot of the relative travel times versus depth for the 220 meter source depth is shown in Figure 3.1. Figure 3.2 displays the plot for the 380 meter source depth. Negative relative travel times in the plots indicate that the overall travel time is less than the reference. These rays arrive at the 200 km horizontal distance before the reference ray.

Since the receiving hydrophones are at set vertical positions (100, 200, 300, 400, and 500 meters), an



interpolation is done to determine relative travel times to them from each source depth. The interpolation program and its listing is in Appendix B. Sometimes more than one R-R ray travels from the source depth to a hydrophone. When this occurs, the ray which arrives first is used in the calculation of relative travel time to that hydrophone.

Equation 2.12 determines the phase shift relating to the relative travel times. The 'A' matrix is formed by taking the appropriate sine and cosine values as in equation 2.24. The 'A' matrix is '40 by 10'.

### C. 'Z' MATRIX

Referring to equation 2.26, the 'Z' matrix is a '40 by 1' column vector. It is the desired beam pattern. The bottom 20 rows give the imaginary terms and are set to zero. The top 20 rows represent the value of the real terms at each source depth. Therefore each of the top 20 rows is set to zero except for the row containing the source. It is set to 1. For example, if the source is at 220 meters then only the top row is set to 1. If the source is at 380 meters then only the ninth row is set to 1.

### D. RESULTING BEAM PATTERN

#### 1. Using the Linear Minimum Variance Method

' $\hat{e}_{LMV}$ ' is calculated using equation 2.47. The resulting beam pattern ' $\hat{z}$ ' is calculated using equation 2.51. The program which calculates the 'A' matrix, uses it in determining ' $\hat{\theta}_{LMV}$ ', and then calculates 'Z' is given in Appendix C. The program listing is also included.



## 2. Using Linear Phase Shifts

The conventional beam pattern is determined by using equation 2.51 where  $\hat{\theta}$  is calculated by approximating the plot of relative travel time vs. depth by a straight line at the receiving hydrophone depths. For example Figure 3.3 represents this plot for the 380 meter source depth. The straight line is determined by a least squares linear regression which minimizes the sum of the squares of the deviations of the actual data points from the straight line of best fit. Note that only data points which are on the dominant curve are used in calculating the straight line. From the straight line, relative travel times to the receiving hydrophones are calculated. The relative travel times for the 380 meter source depth are given in Table I. They correspond to a plane wave arrival angle of 3.73 degrees.  $\hat{\theta}$  is determined by converting these relative travel times to phase delays using equation 2.12 and then taking the appropriate sine and cosine values of these phase delays as in equation 2.24. The amplitude weights are initially assumed to be unity.

A second method for obtaining the conventional beam pattern is calculated by the same procedure except the amplitude weights which are determined by equation 2.50, the  $\hat{\theta}_{LMV}$  amplitude weights, are applied to each hydrophone.



TABLE I

Relative Travel Times For 380 Meter Source Depth

<u>Hydrophone Depth</u>	<u>Relative Travel Time</u>
100 meters	-0.07565509 sec.
200 meters	-0.07131599 sec.
300 meters	-0.06697690 sec.
400 meters	-0.06263780 sec.
500 meters	-0.05829871 sec.





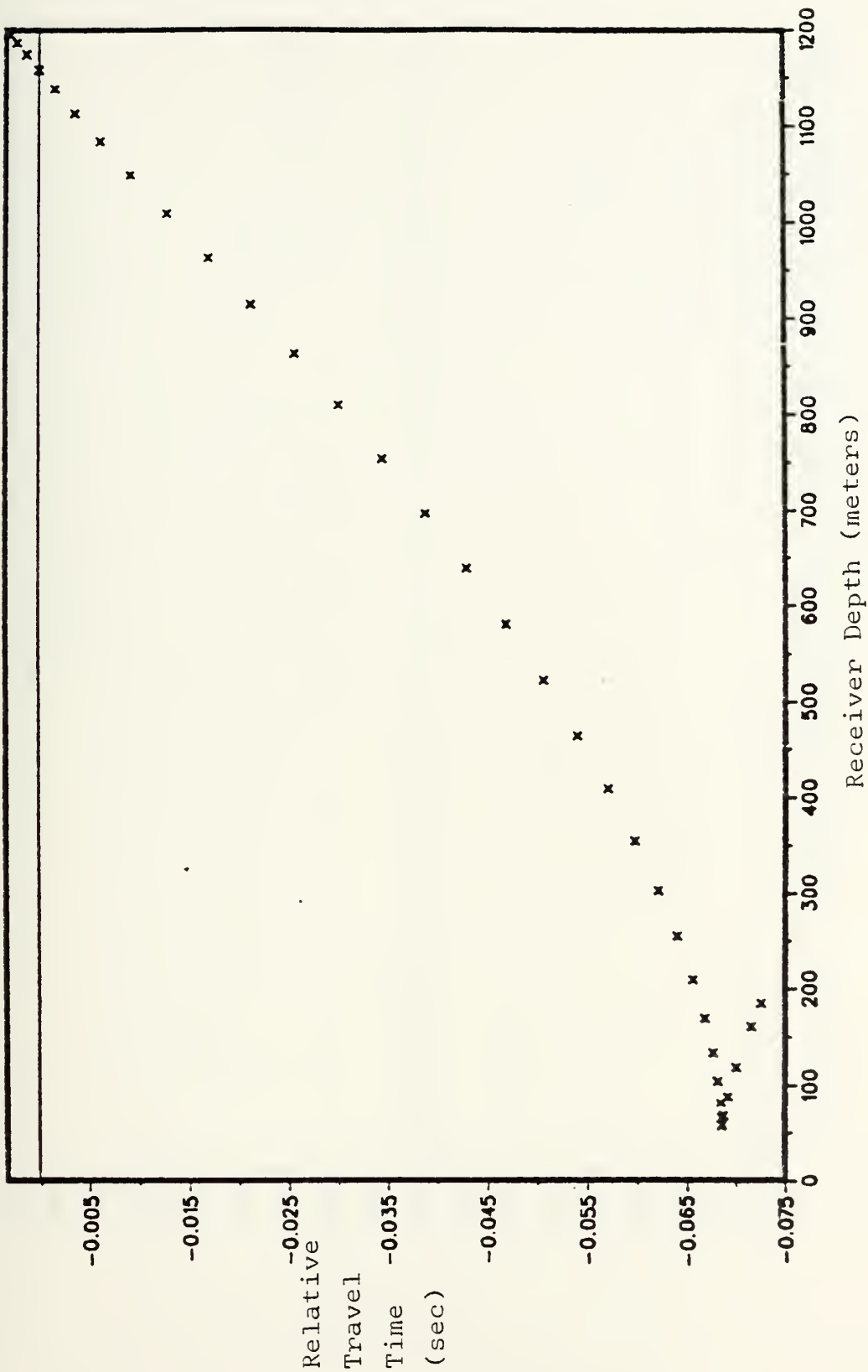


Figure 3.1 Relative Travel Time vs. Depth (220 meter source)



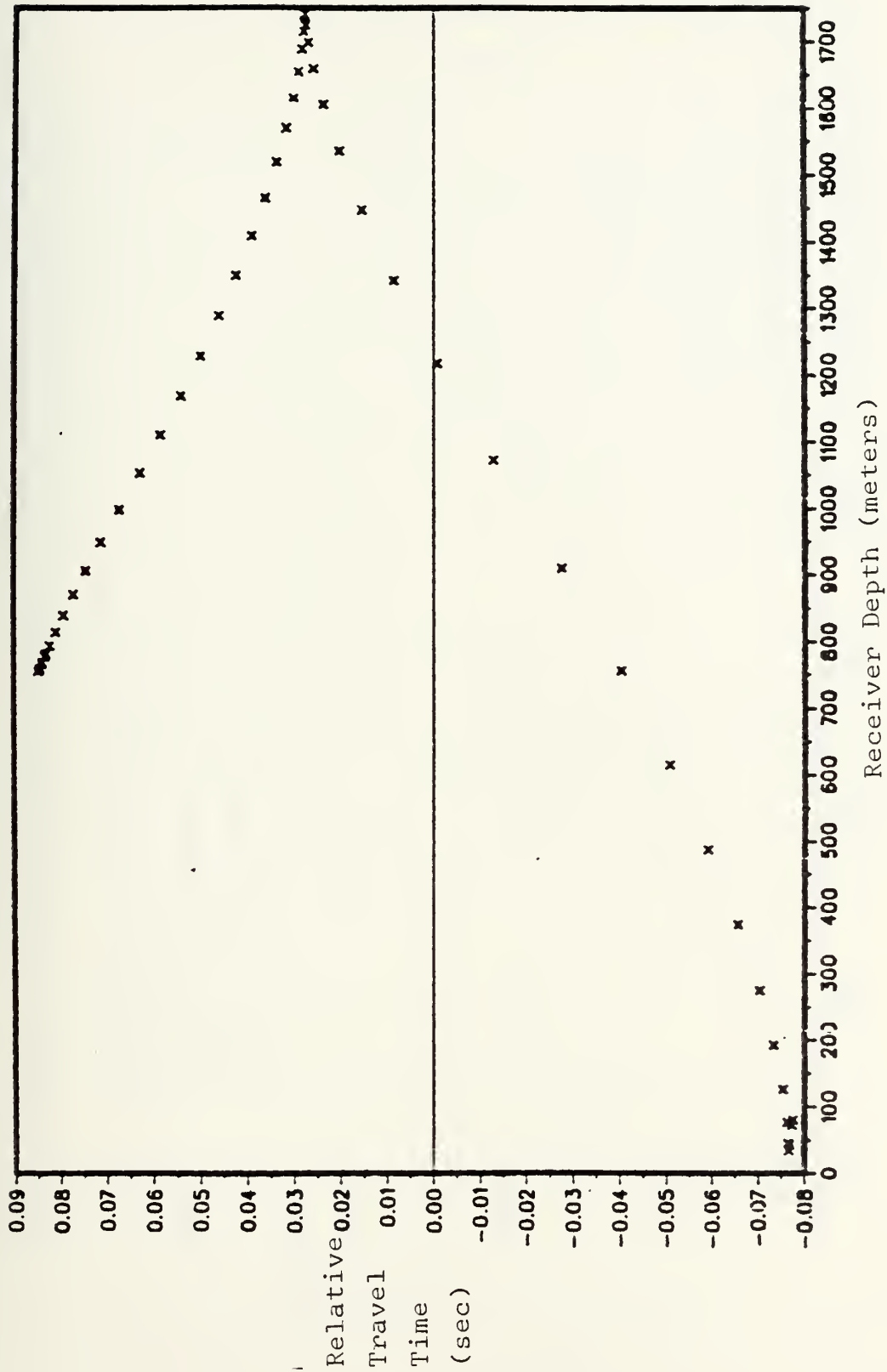


Figure 3.2 Relative Travel Time vs. Depth (380 meter source)



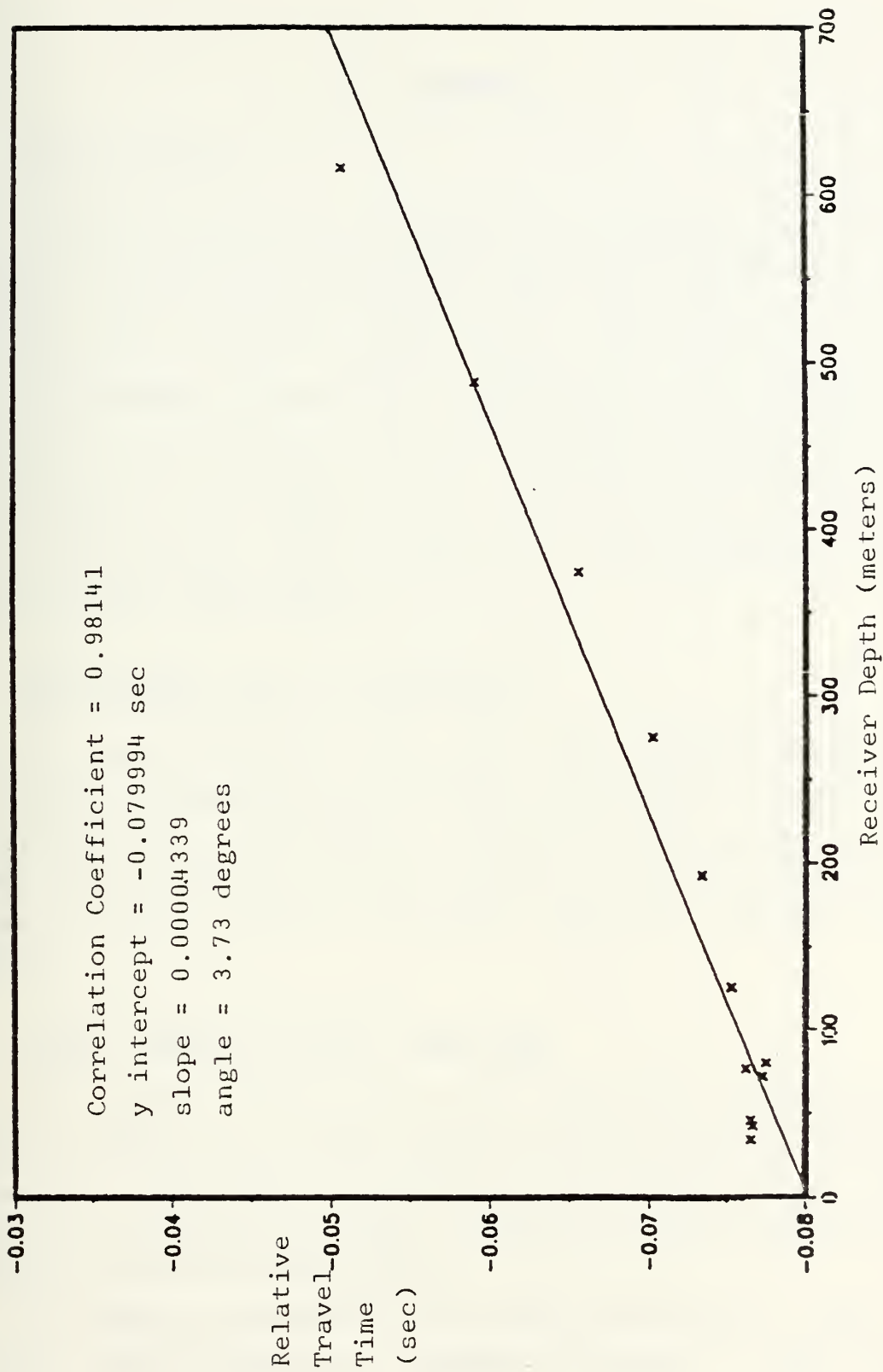


Figure 3.3 Straight Line Approx. of Rel. Trav. Time vs. Depth (source at 380 m)



## IV. RESULTS

### A. EXACT SOLUTION

An exact solution is derived for the beam pattern if the number of receiving hydrophones equal the number of source depths. For example, when the 5 receivers are used to discriminate between 5 source depths (220, 240, 260, 280, and 300 meters) there are 10 equations with 10 unknowns. Figure 4.1 is a plot of the resulting beam pattern with the source at the shallowest depth. Note that because of round-off errors in the 'IMSL' subroutines there is a small value for the resulting beam pattern at the non-energy source depths under investigation.

### B. FOUR DEPTHS WITH TWO RECEIVERS

For source depths at 220, 280, 300, and 320 meters with receiving hydrophones at 100 and 200 meters, there are 8 equations with 4 unknowns. Figure 4.2 is a plot of the resulting beam pattern with a source at the 220 meter depth. Figure 4.3 is the plot for the source at the 280 meter depth.

### C. TWENTY DEPTHS WITH TWO RECEIVERS

For all 20 source depths with receiving hydrophones at 100 and 200 meters, there are 40 equations with 4 unknowns. Figure 4.4 is a plot of the resulting beam pattern for a source at the 220 meter depth. Figure 4.5 is a plot for the source at the 380 meter depth.

In order to determine if the ' $\hat{\theta}$ ' calculated in this case is the best an alternate method is devised. Four source





depths (220, 240, 260 meters, and another source test depth) with the original source at the 220 meter depth and receivers at 100 and 200 meters are used. The beam pattern is calculated each time with a different source test depth substituted for the fourth source depth. The 5 best resulting beam patterns are selected along with the 8 source depths (220, 240, 260 meters, and the 5 test depths which created the 5 best beam patterns). Then, using these 8 source depths, ' $\hat{\theta}$ ' is determined for the two receivers. This ' $\hat{\theta}$ ' is applied to the two receivers and the beam pattern obtained for all 20 source depths.

The resulting beam pattern obtained by this alternate method isn't as good as the beam pattern obtained by using all 20 source depths in the determination of ' $\hat{\theta}$ '.

#### D. TWENTY DEPTHS WITH FIVE RECEIVERS

For all 20 source depths with all 5 receiving hydrophones there are 40 equations with 10 unknowns. Figure 4.6 is a plot of the resulting beam pattern with the source at the 220 meter depth. Figures 4.7, 4.8, and 4.9 are the plots for the source at the 360, 380, and 400 meter depths respectively.

#### E. CONVENTIONAL BEAMFORMER

Figure 4.10 is a plot of the beam pattern for a conventional beamformer using linear phase shifts across the array with the source at the 380 meter depth and the amplitude weights set to unity. All 20 source depths and 5 receiving hydrophones are used. Note that in figure 4.10 that there is less than 1 db discrimination between each of the source depths. Figure 4.11 is the plot obtained for the amplitude weights set to values determined by equation 2.50.



## F. RANGE OF 250 KILOMETERS

The calculations were repeated for a range of 250 km using the same 20 source depths and 5 receiving hydrophones. Figures 4.12 and 4.13 represent the plots of relative travel times versus depth for the 220 and 380 meter source depths respectively. Figure 4.14 represents the straight line approximation of the relative travel times for the 380 meter depth. Note that in this figure the relative travel times are represented by two straight lines; the upper line represents linear phase shifts of the slower travel times for the conventional beamformer while the lower line represents linear phase shifts of the faster travel times. Tables II and III are the straight line interpolations of these slower and faster travel times which correspond to arrival angles of 4.04 and -3.16 degrees respectively. Figures 4.15 and 4.16 are the resulting beam patterns for the conventional beamformer for the slower travel times using unity amplitude weights and linear minimum variance amplitude weights respectively. Figures 4.17 and 4.18 are the beam patterns for the faster travel times.

Figures 4.19, 4.20, 4.21, and 4.22 represent plots of the beam pattern for the source at the 220, 340, 360, and 380 meter depths respectively.



TABLE II

Slower Ray Travel Times For 250 km Range and 380 m Source

<u>Hydrophone Depth</u>	<u>Relative Travel Time</u>
100 meters	-0.09949109 sec.
200 meters	-0.09478615 sec.
300 meters	-0.09008121 sec.
400 meters	-0.08537627 sec.
500 meters	-0.08067133 sec.

TABLE III

Faster Travel Times For 250 km Range and 380 m Source

<u>Hydrophone Depth</u>	<u>Relative Travel Time</u>
100 meters	-0.10100745 sec.
200 meters	-0.10468763 sec.
300 meters	-0.10836781 sec.
400 meters	-0.11204799 sec.
500 meters	-0.11572817 sec.



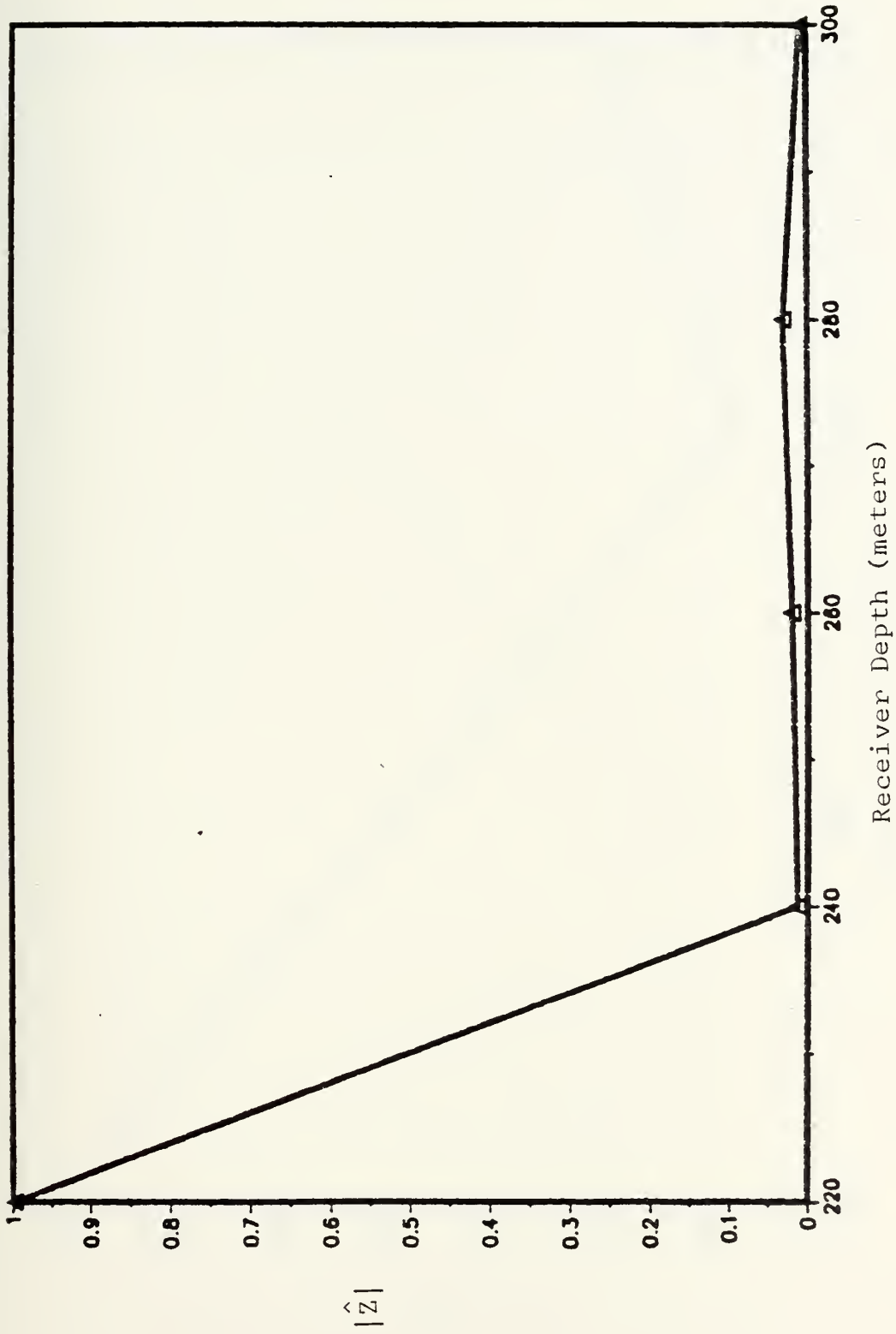


Figure 4.1 Beam Amplitude vs. Source Depth (5 depths 5 receivers)





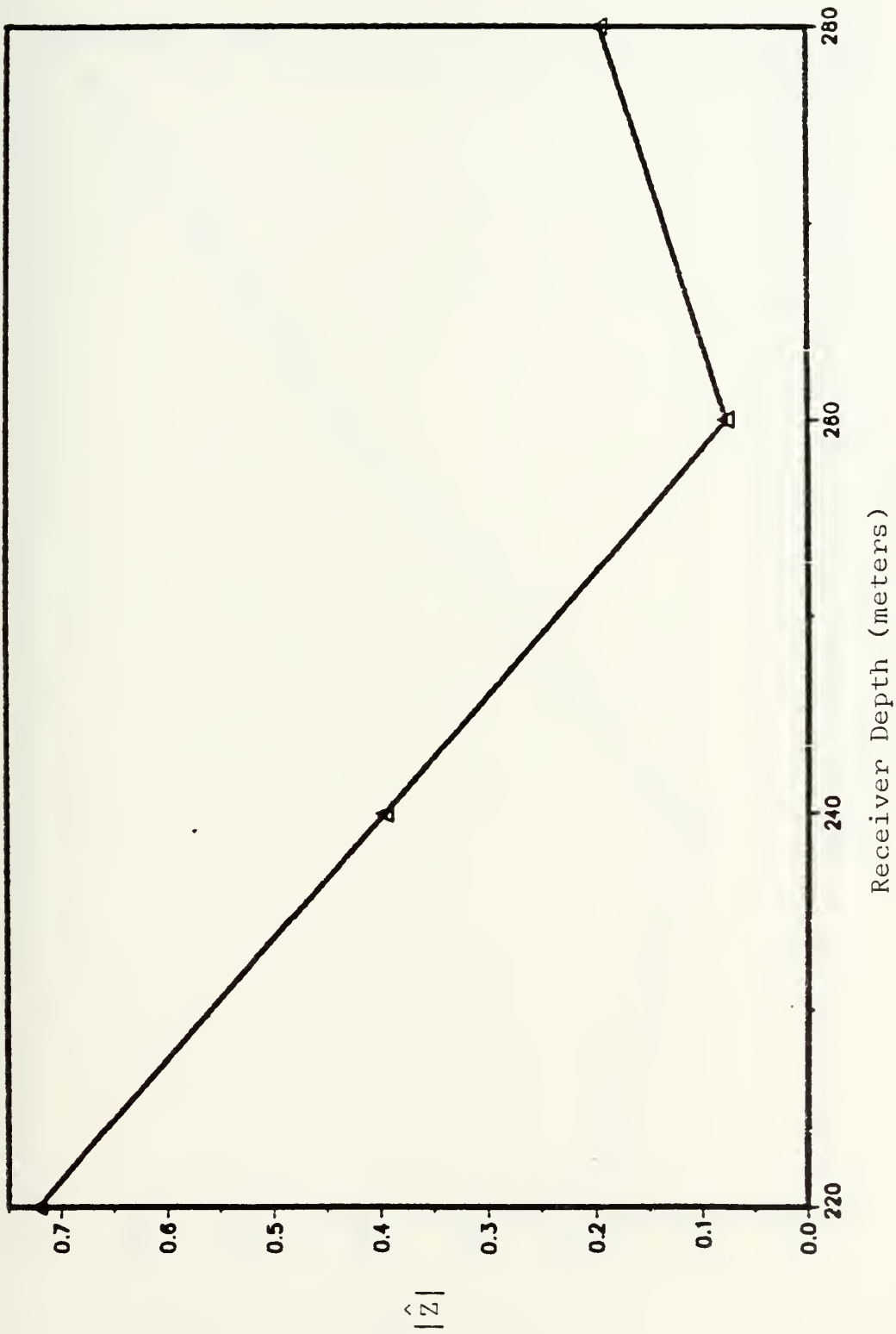


Figure 4.2 Beam Pattern (4 depths 2 receivers, source at 220 m)



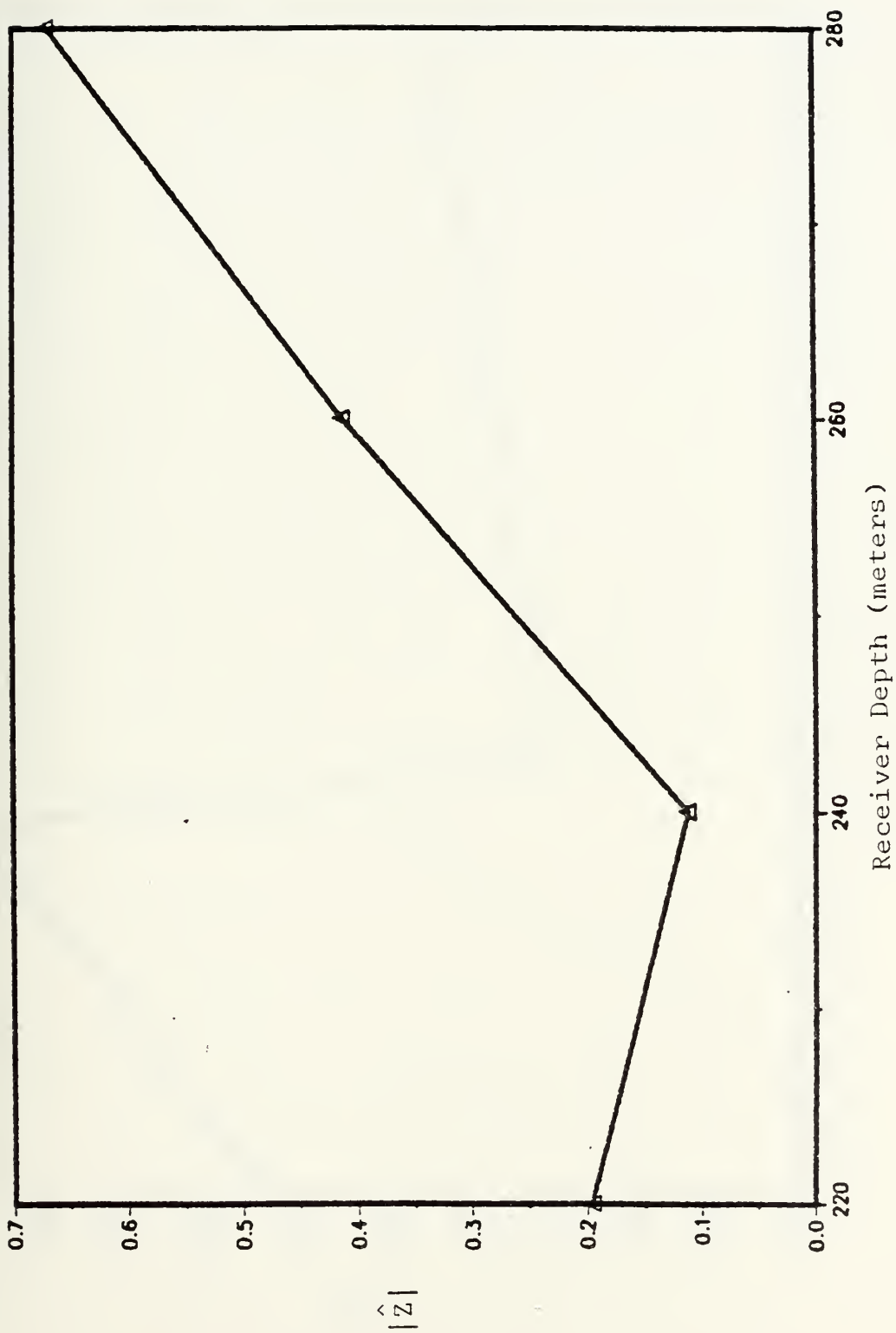


Figure 4.3 Beam Pattern (4 depths 2 receivers, source at 280 m)



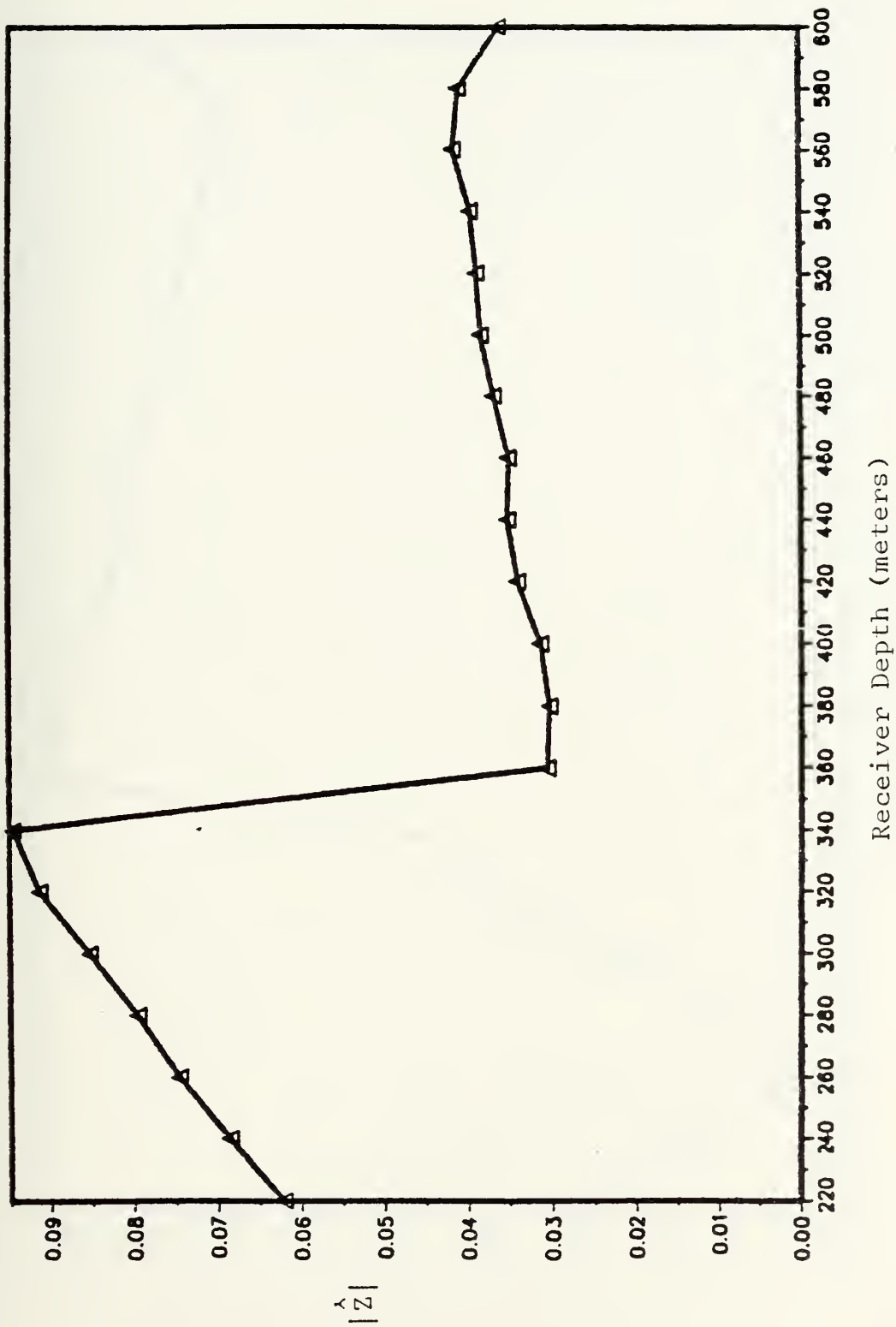


Figure 4.4 Beam Pattern (20 depths 2 receivers, source at 220 m)



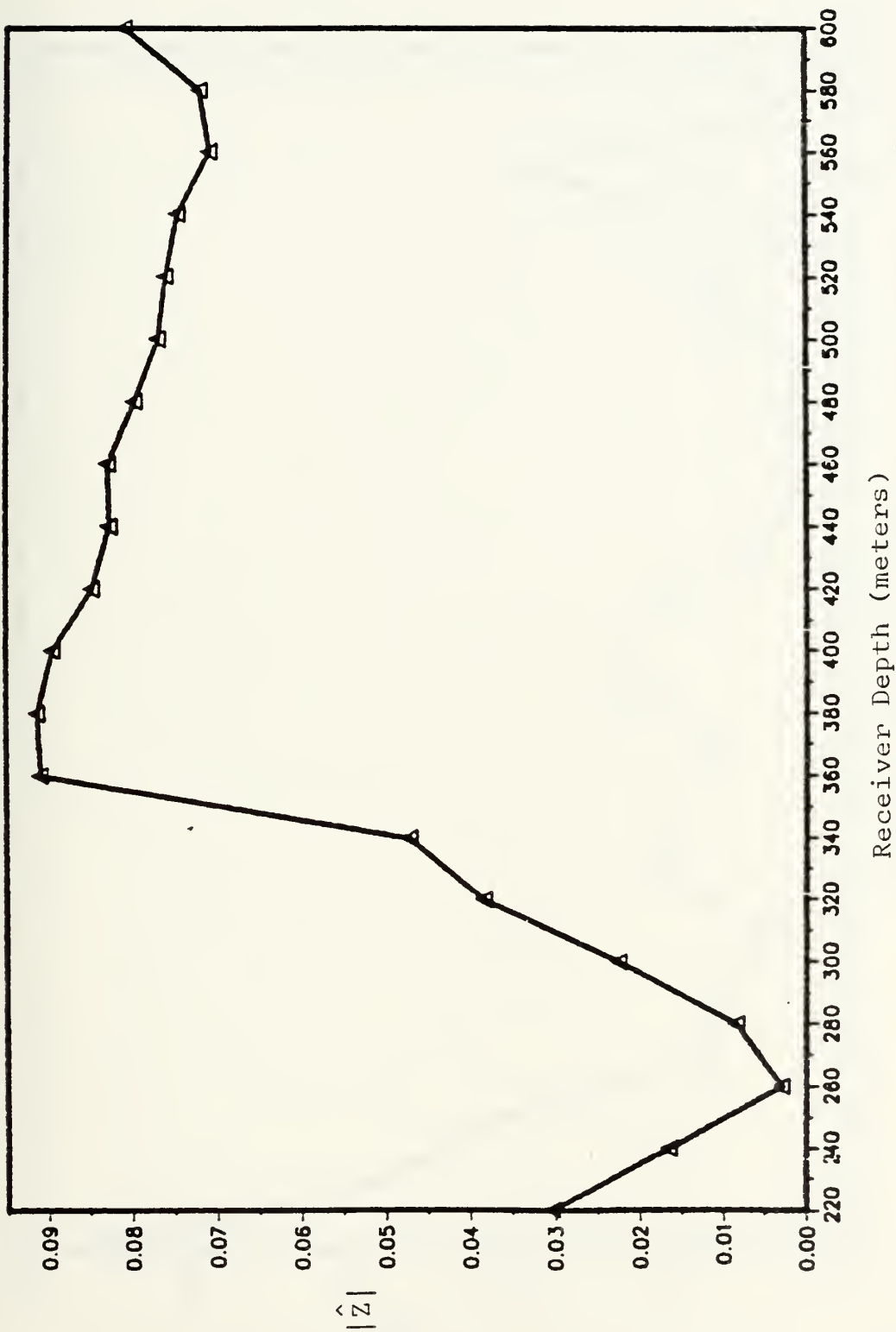


Figure 4.5 Beam Pattern (20 depths 2 receivers, source at 380 m)





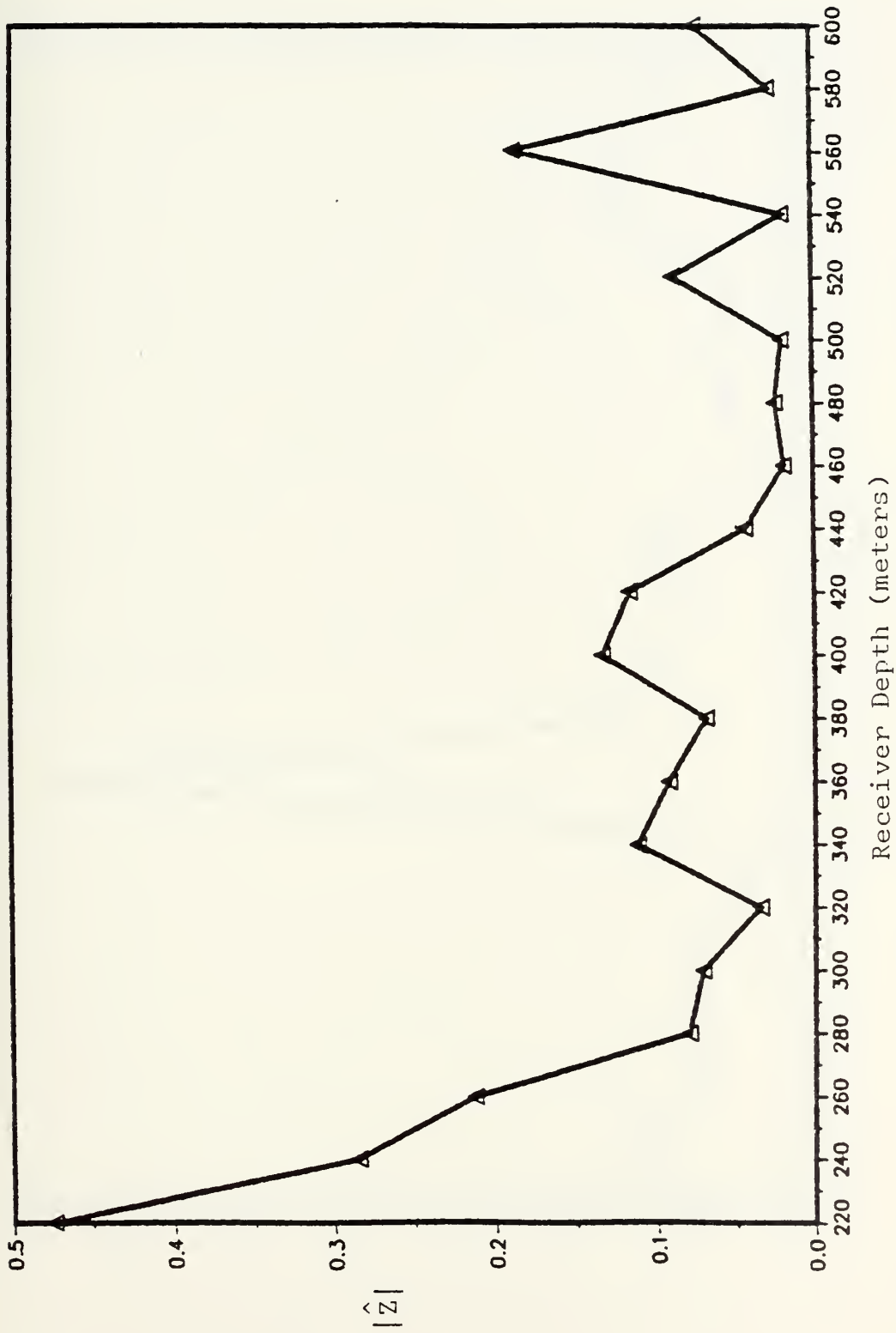


Figure 4.6 Beam Pattern (20 depths 5 receivers, source at 220 m)



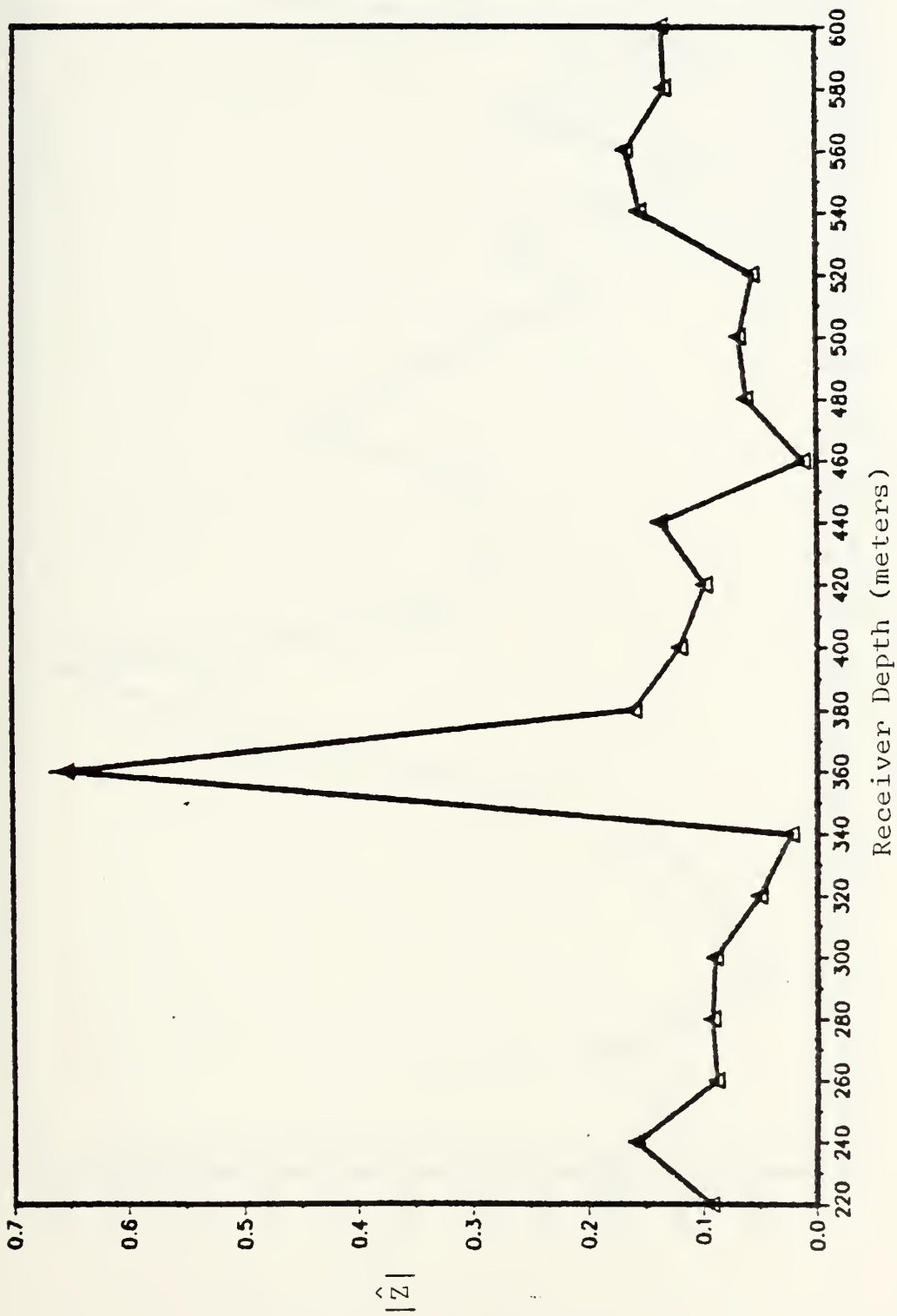


Figure 4.7 Beam Pattern (20 depths 5 receivers, source at 360 m)



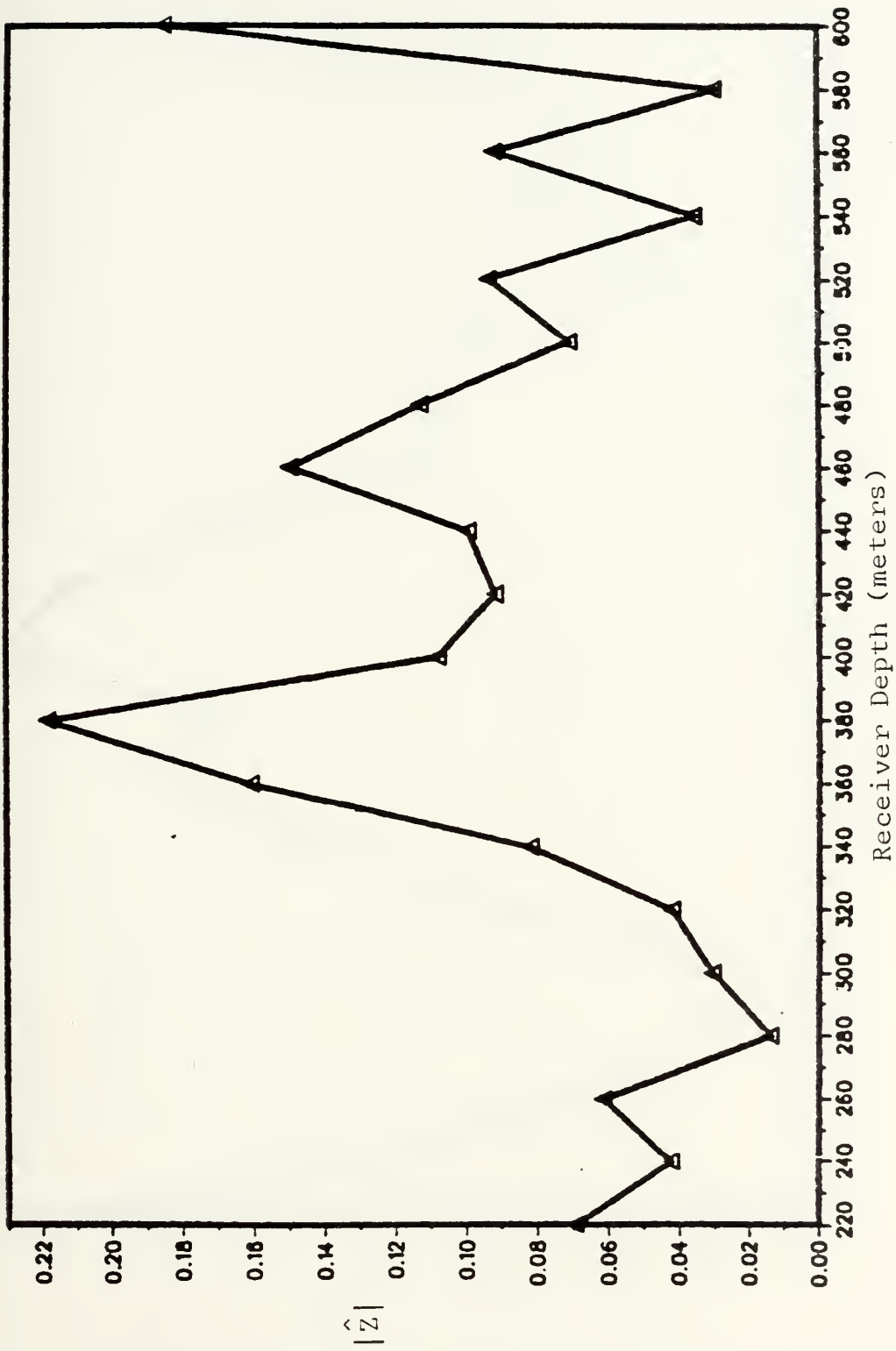


Figure 4.8 Beam Pattern (20 depths 5 receivers, source at 380 m)



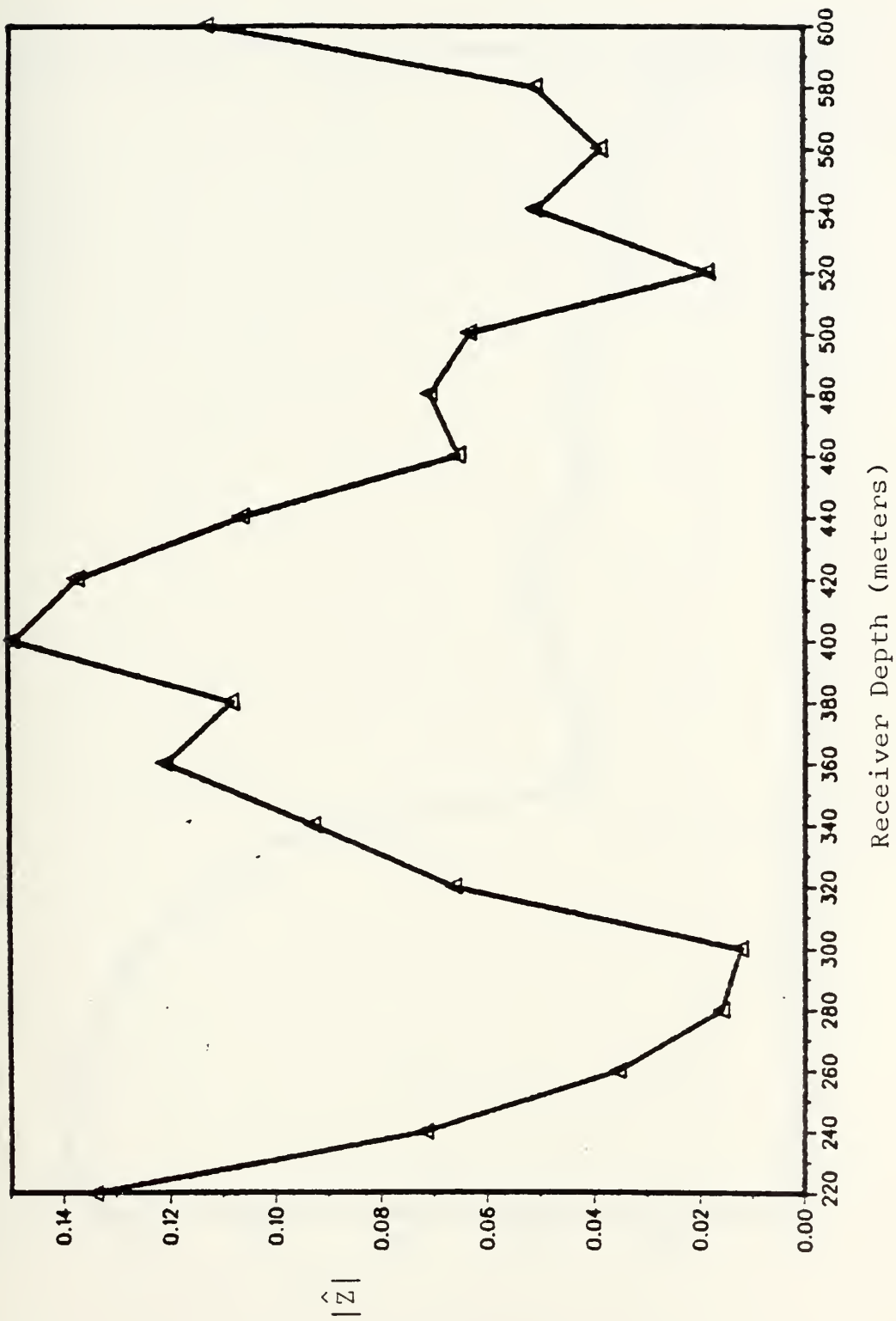


Figure 4.9 Beam Pattern (20 depths 5 receivers, source at 400 m)





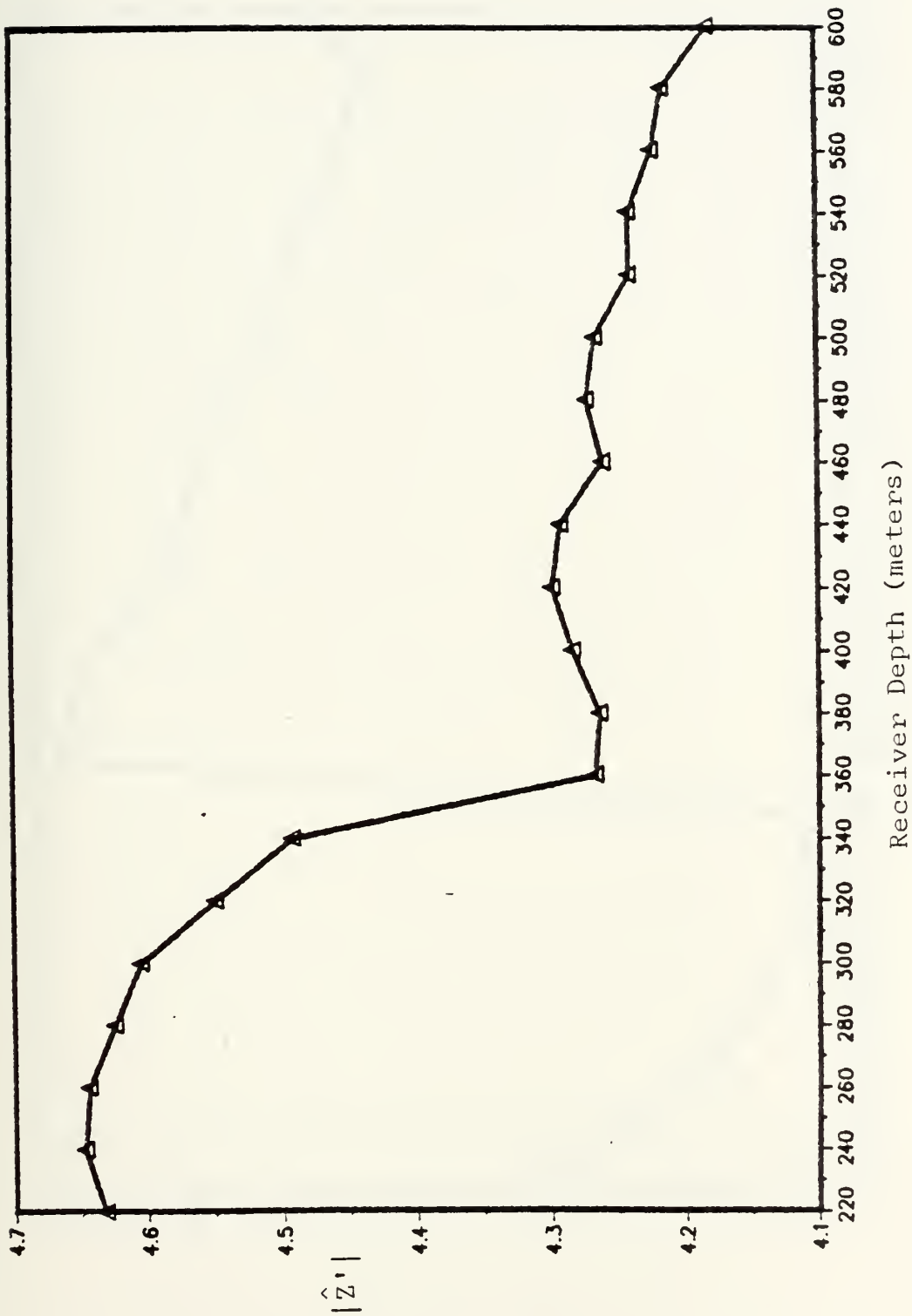


Figure 4.10 Conventional Beam Pattern (source at 380 meters)



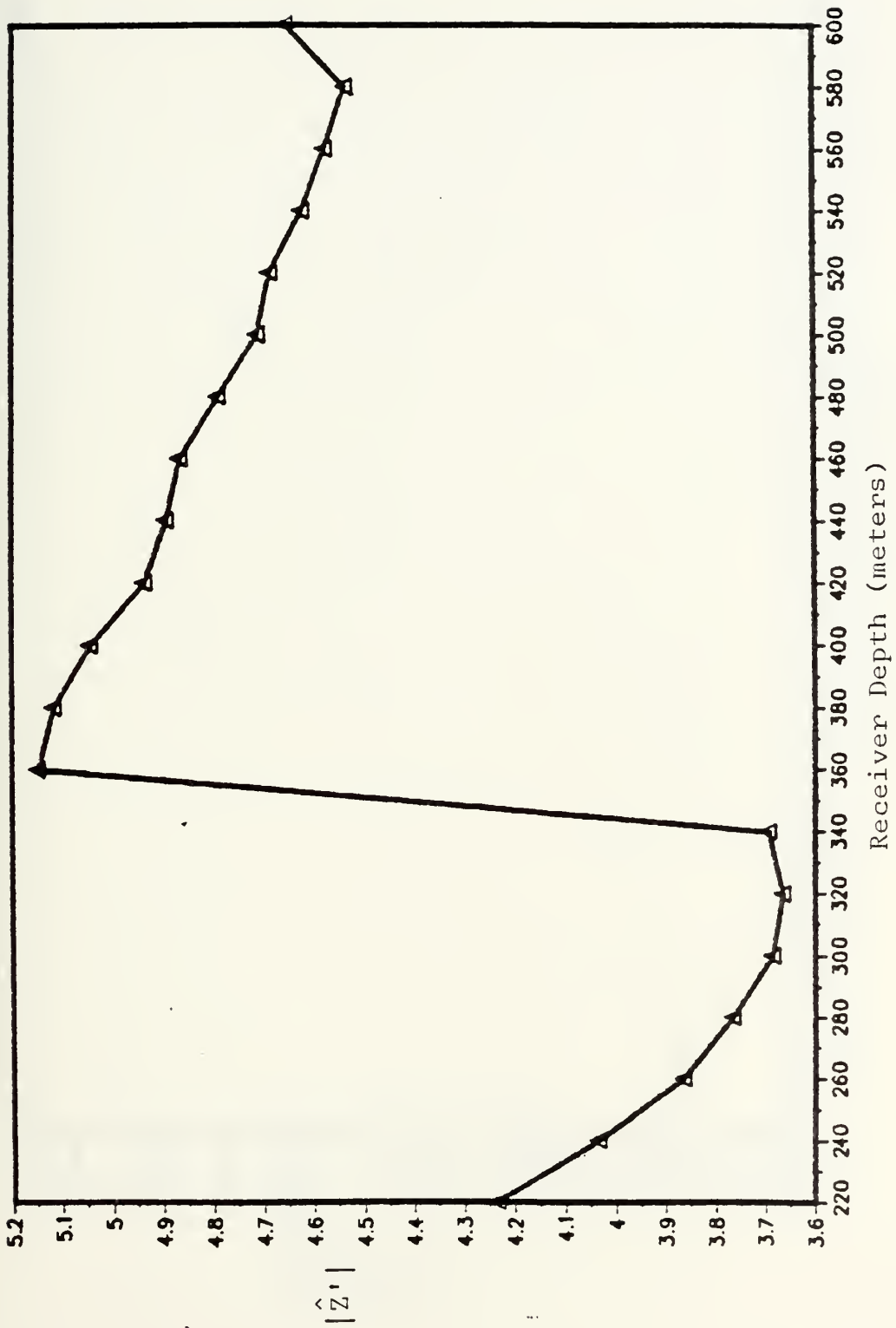


Figure 4.11 Conventional Beam Pattern (non-unity amp. wts. source at 380 m)



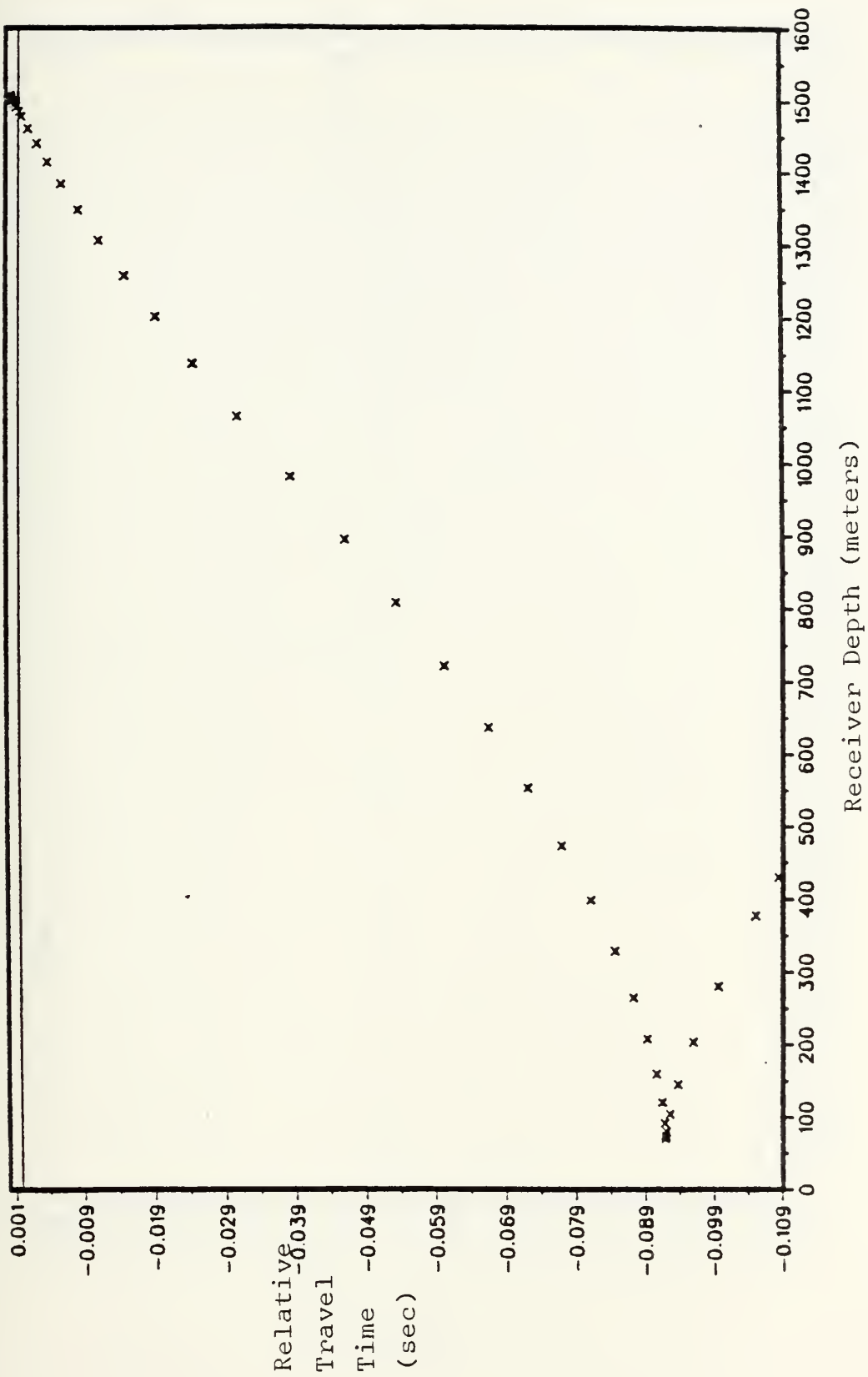


Figure 4.12 Relative Travel Time vs. Depth (range=250 km, source at 220 m)



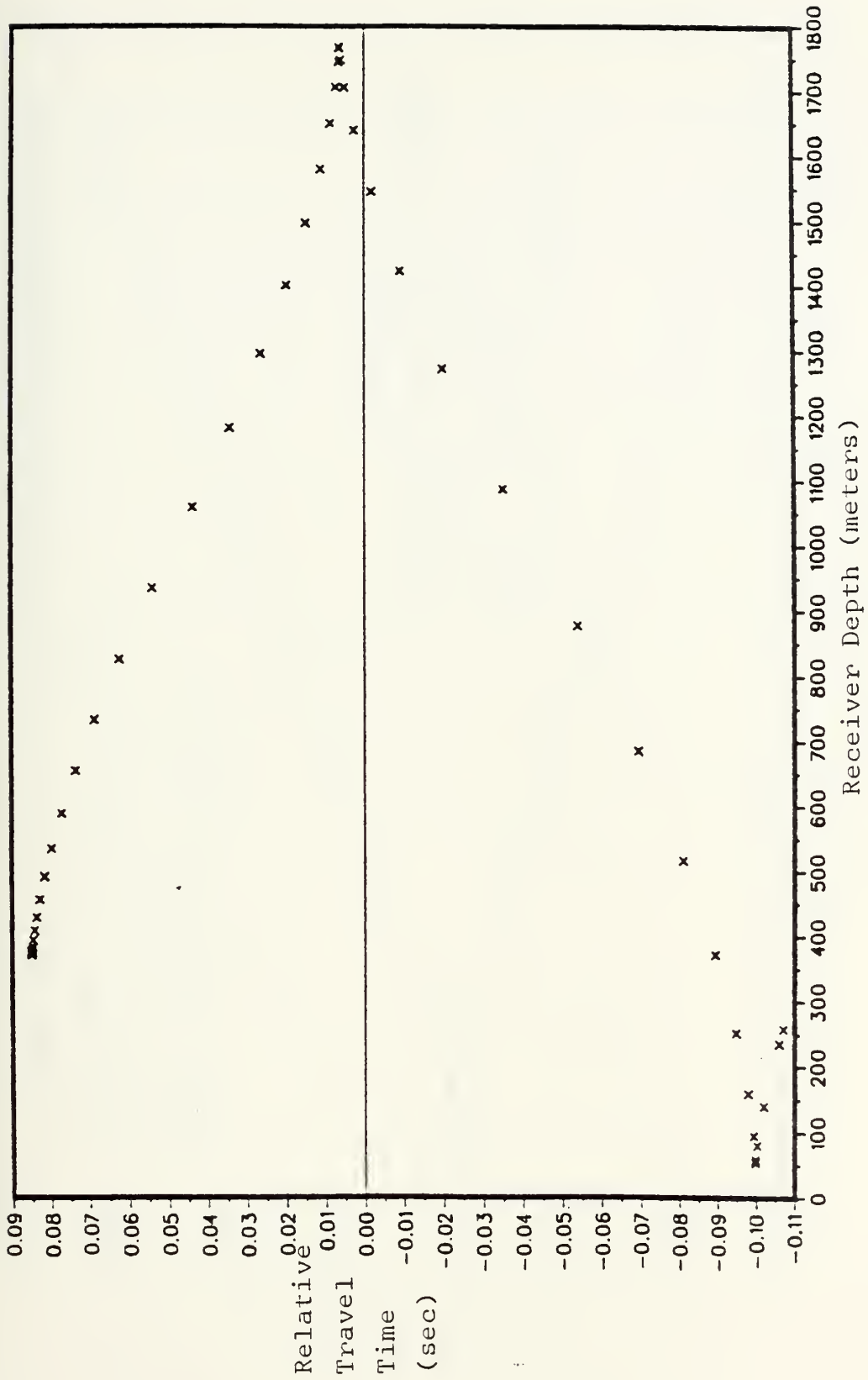


Figure 4.13 Relative Travel Time vs. Depth (range=250 km, source at 380 m)





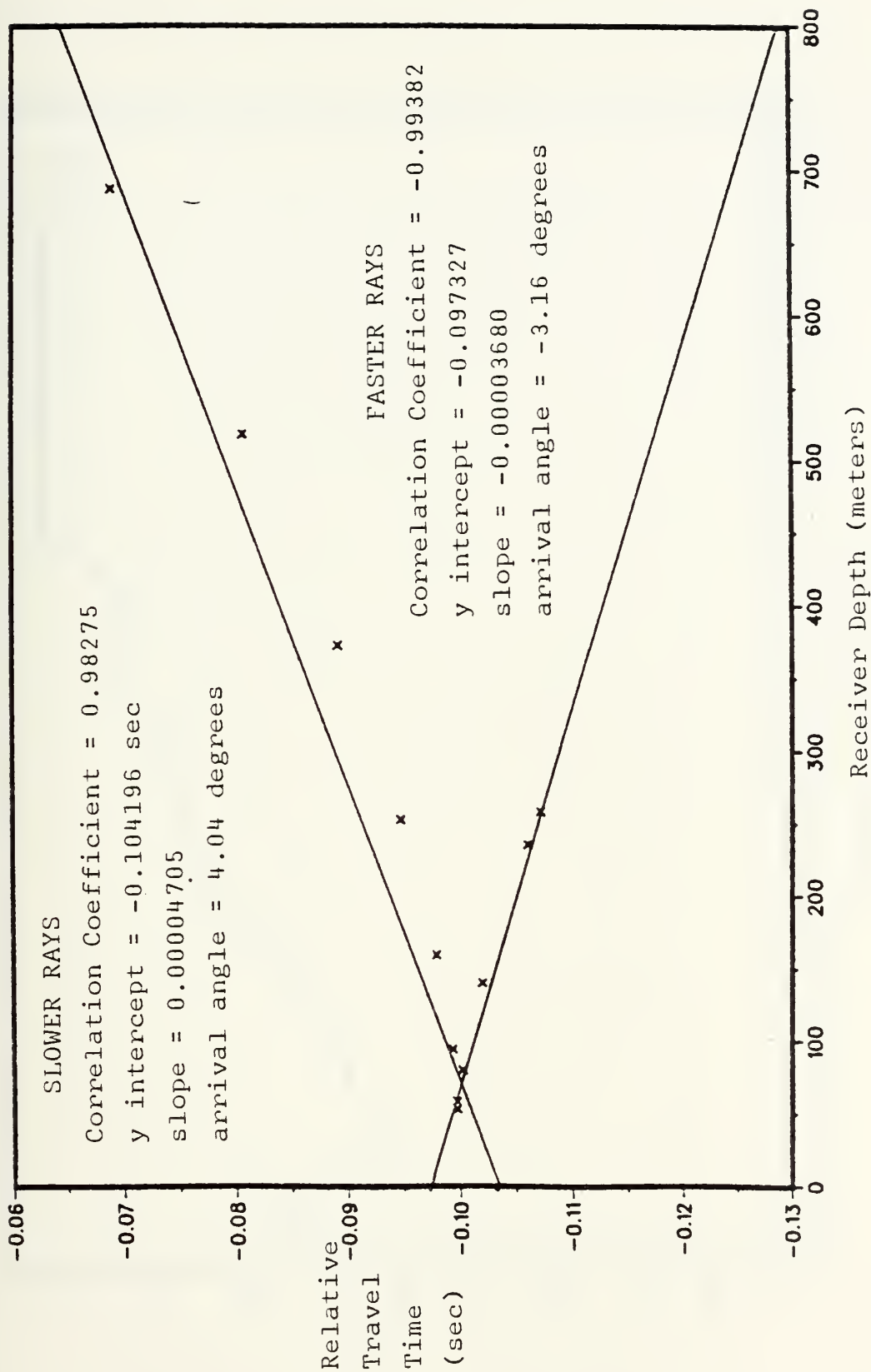


Figure 4.14 St. Line Approx. of Rel. Trav. Time vs. Depth (R=250 km, d=380 m)



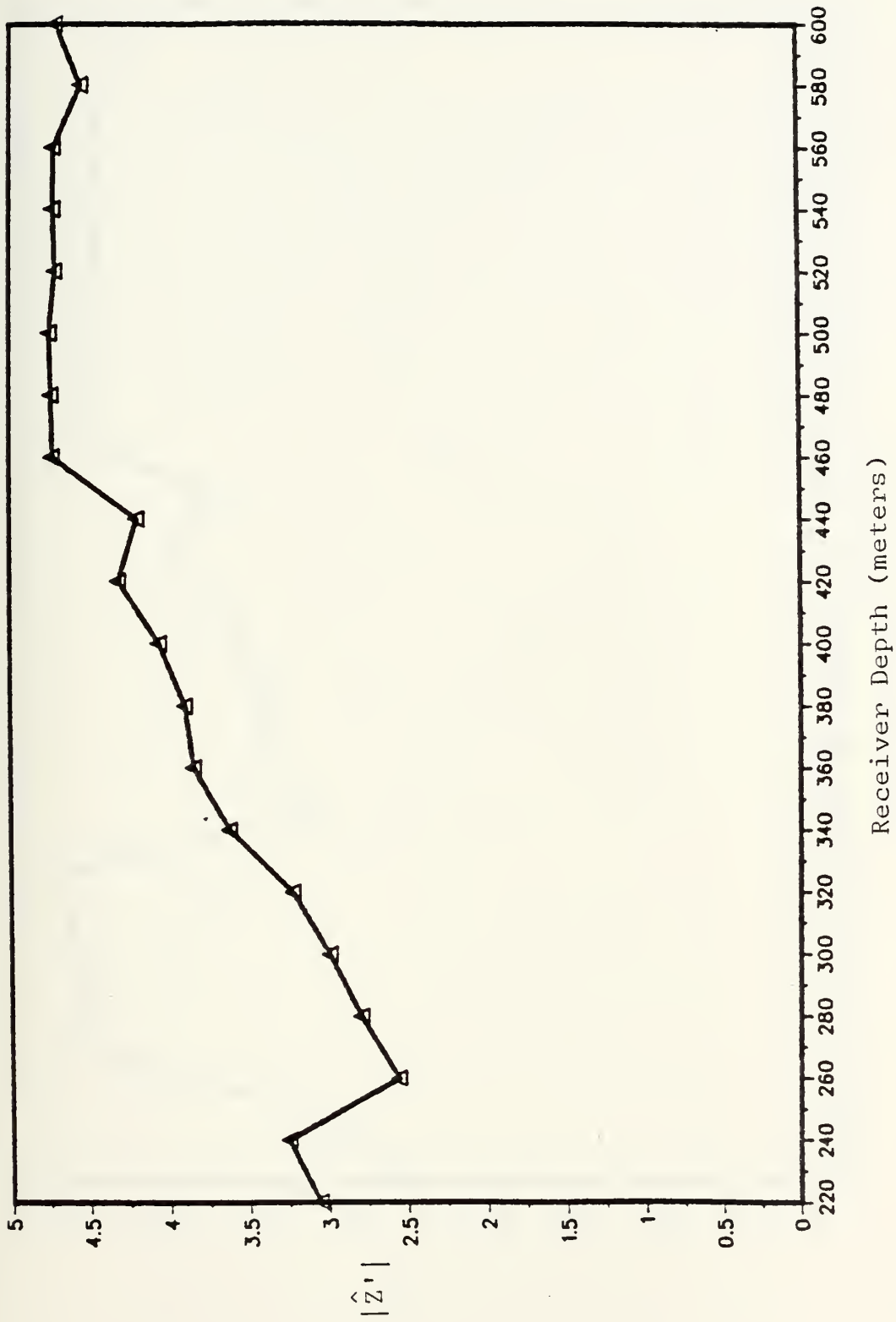


Figure 4.15 Conventional Beam Pattern ( $R=250$  km,  $d=380$  m, slower times,  $a=1$ )



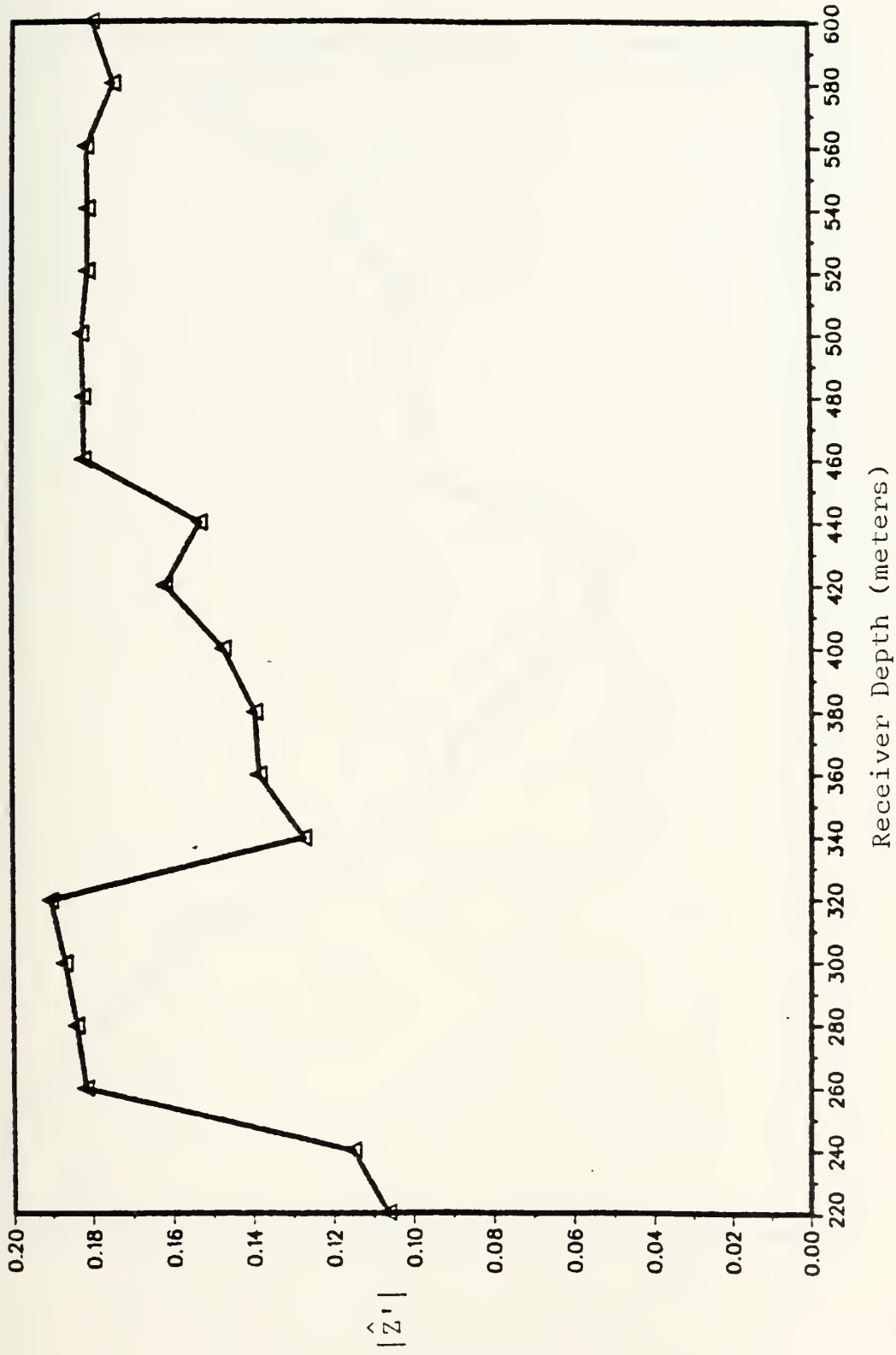


Figure 4.16 Conventional Beam Pattern (R=250 km, d=380 m, slower times, LMV a)



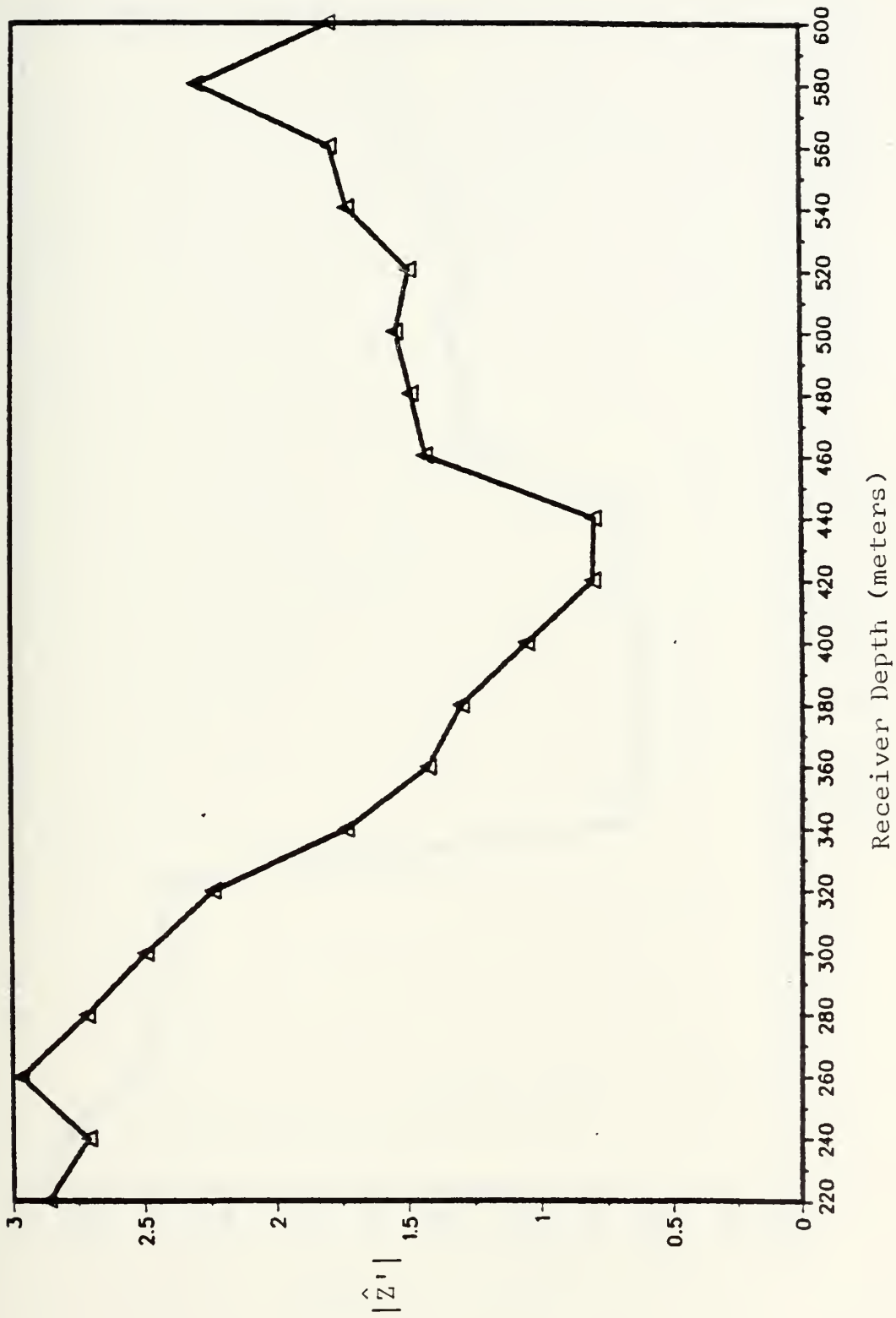


Figure 4.17 Conventional Beam Pattern ( $R=250$  km,  $d=380$  m, faster times,  $a=1$ )





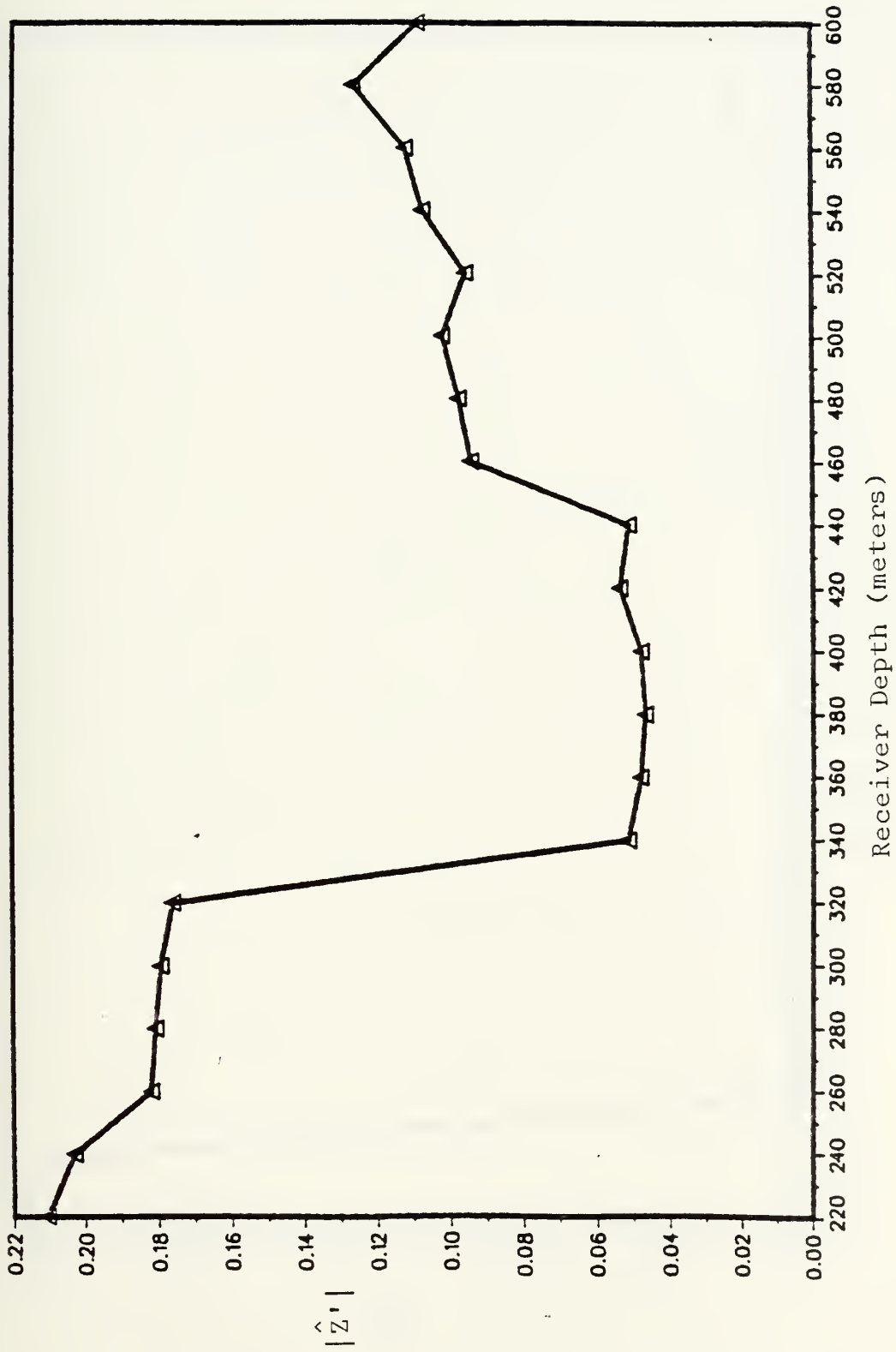


Figure 4.18 Conventional Beam Pattern ( $R=250$  km,  $d=380$  m, faster times, LMV a)



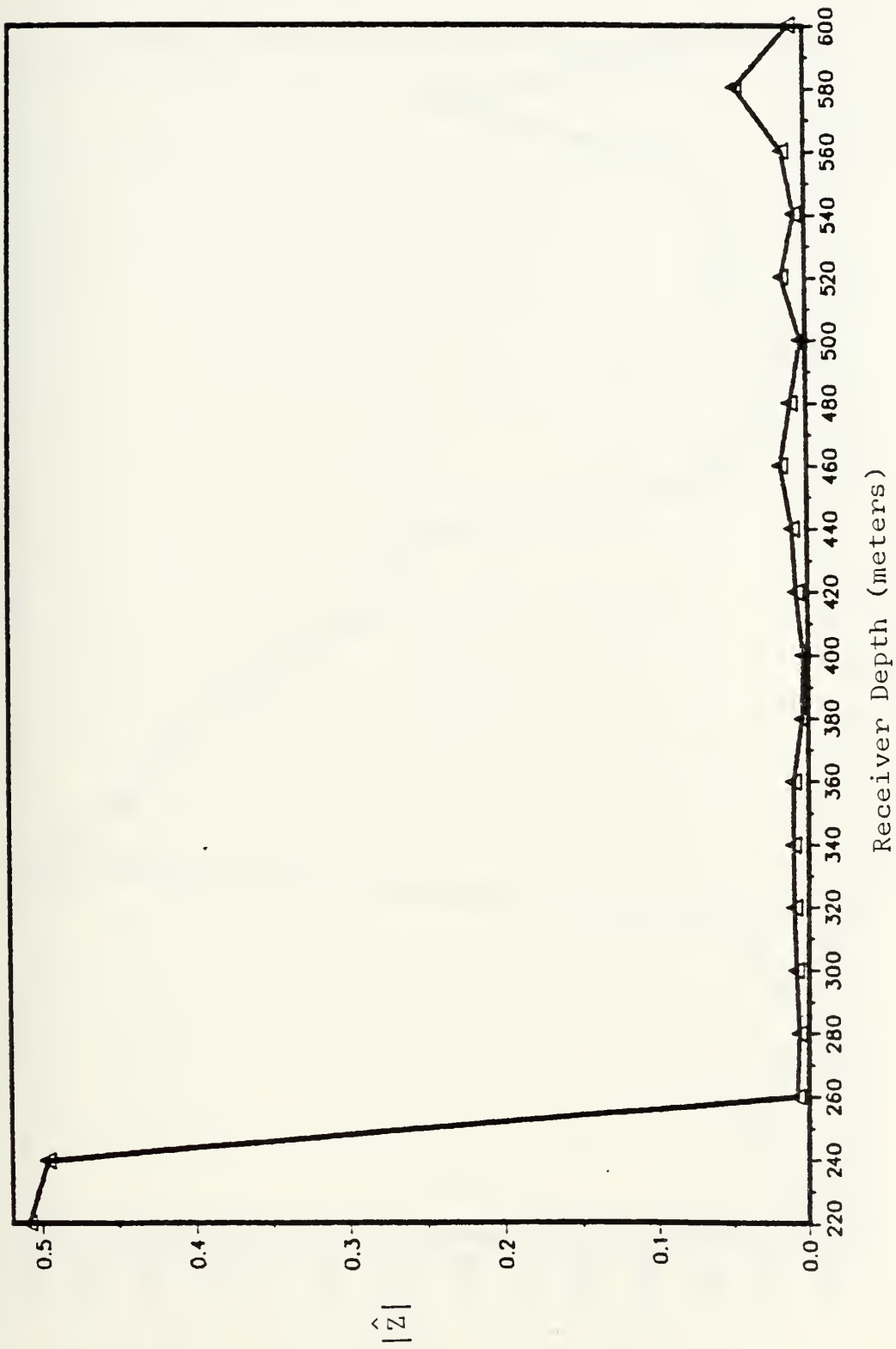


Figure 4.19 Beam Pattern (R=250 km, 20 depths, 5 receivers, 5 receivers, source at 220 m)



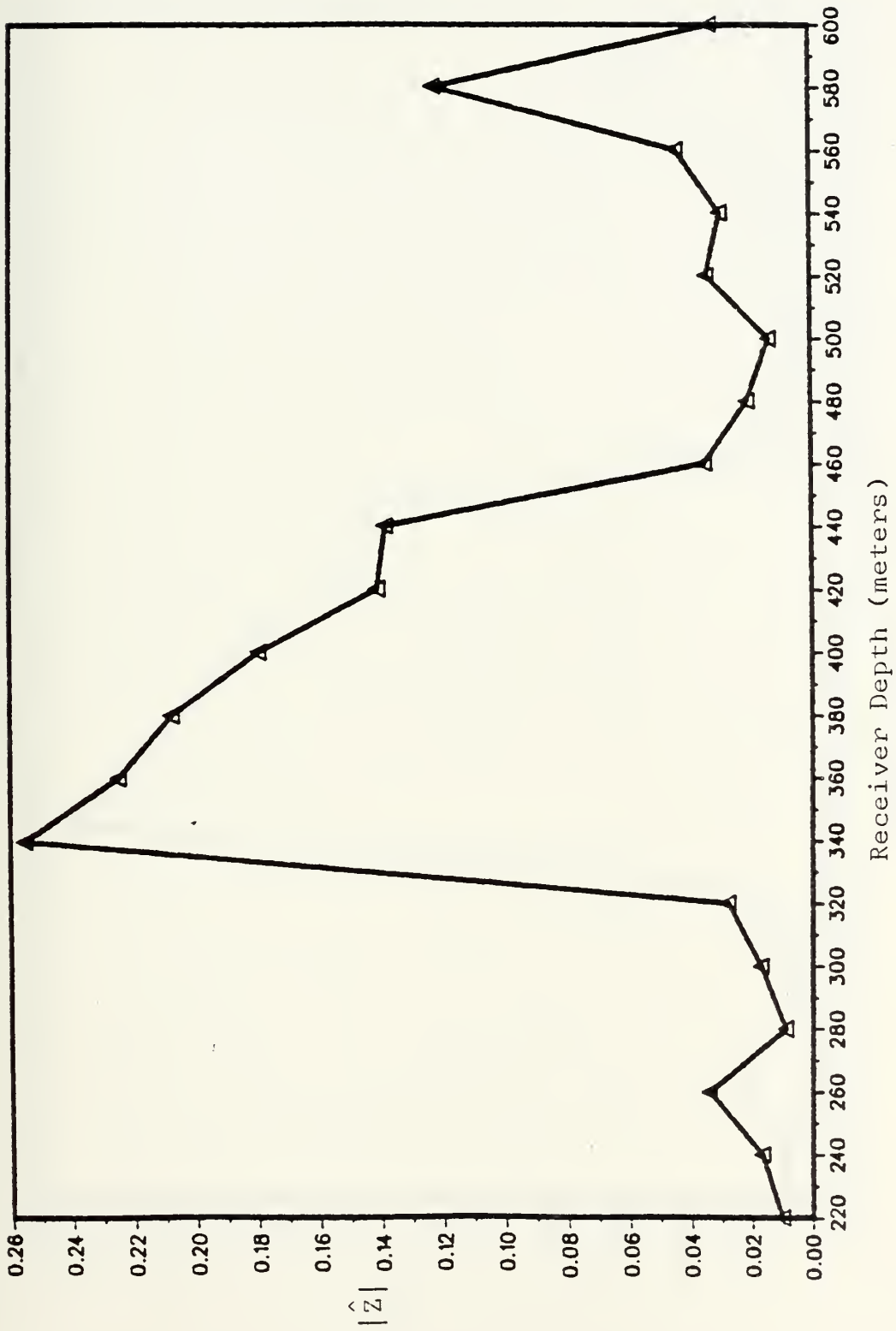


Figure 4.20 Beam Pattern ( $R=250$  km, 20 depths, 5 receivers, source at 340 m)



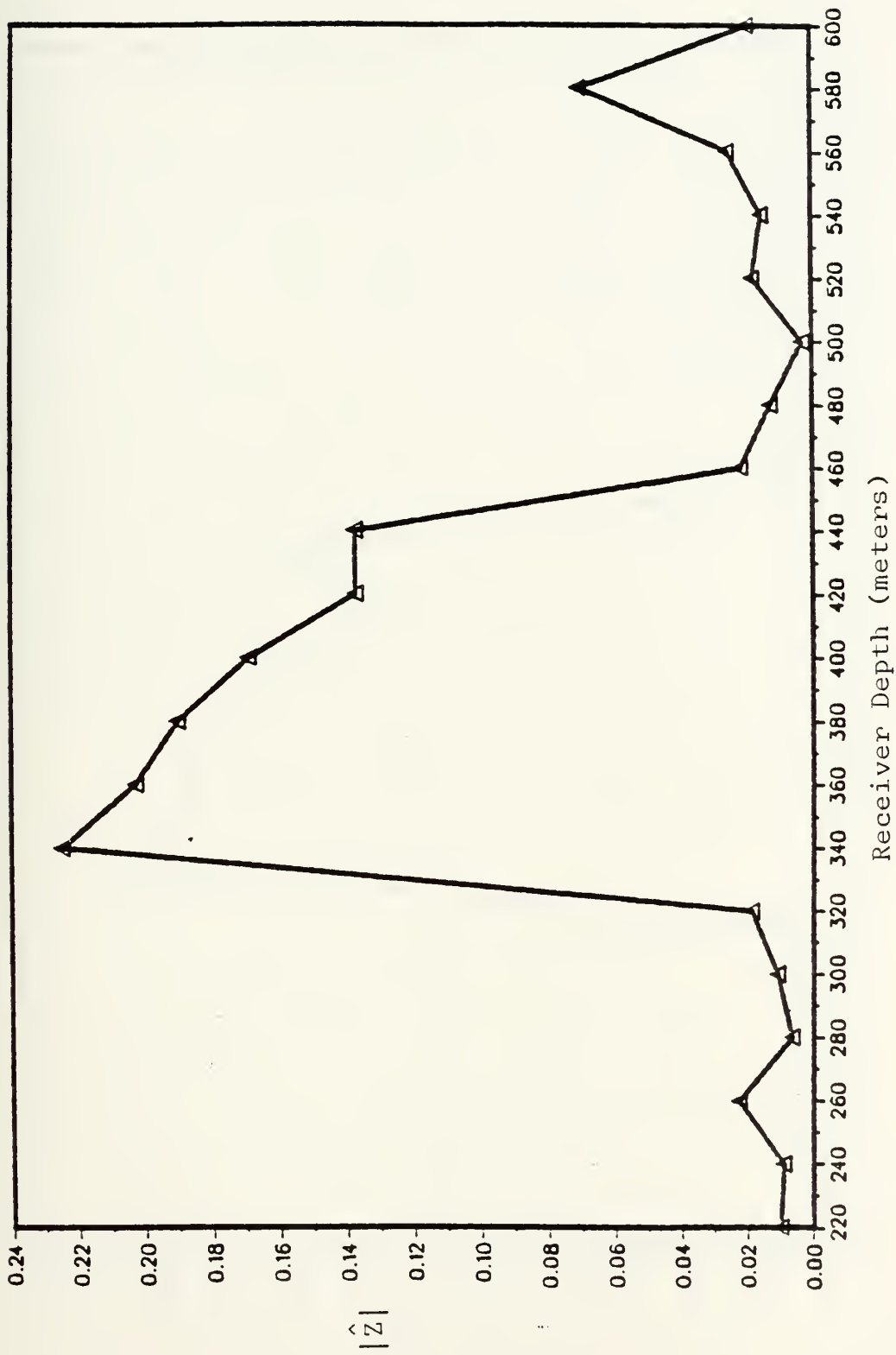


Figure 4.21 Beam Pattern (R=250 km, 20 depths, 5 receivers, source at 360 m)





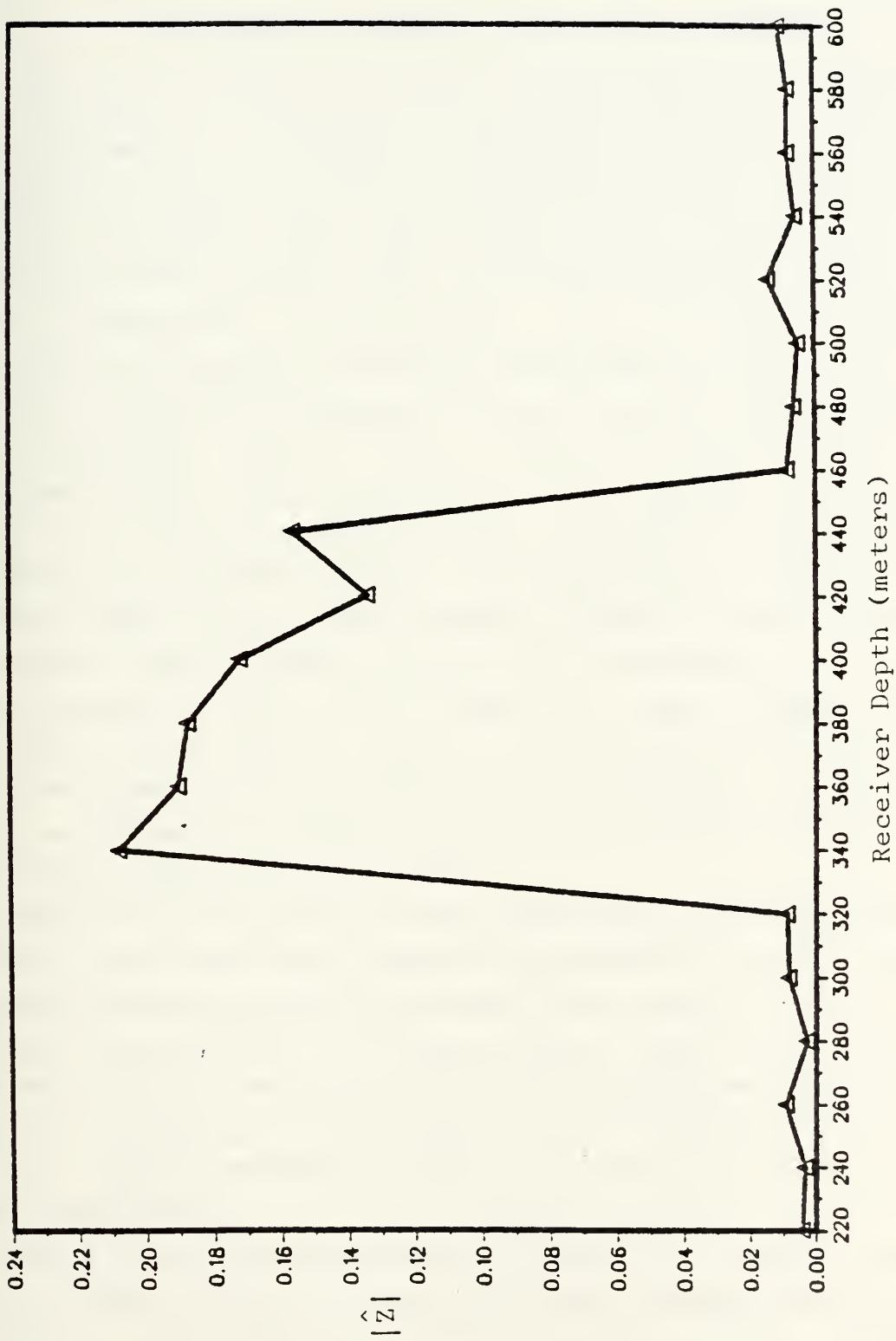


Figure 4.22 Beam Pattern ( $R=250$  km, 20 depths, 5 receivers, source at 380 m)



## V. DISCUSSION OF RESULTS AND RECOMMENDATIONS

For many of the cases examined, the linear minimum variance estimation technique gives high resolution in the "depth beam pattern" for sources at long range. Figures 4.2 and 4.3 represent beam patterns for four depths with two receivers where the main lobe is at the desired source depth with a beamwidth of 30 meters. For 20 depths with 2 receivers the system is highly overdetermined and the beam pattern portrayed in figure 4.4 has its main lobe 80 meters from the source depth. At the source depth the strength of the beam pattern is 3.6 db down. For figure 4.5 the main lobe is on the source depth with a beamwidth of 250 meters.

For all 20 source depths with 5 hydrophone receivers the results range from a beam pattern having its main lobe on the source depth (figure 4.7) with a beamwidth of 20 meters and a secondary lobe 12.1 db down to a beam pattern having its main lobe 40 meters from the source depth (figure 4.22). For the beam pattern in figure 4.22 the width of the main lobe is 80 meters and the strength of the beam pattern at the source depth is 0.8 db down.

When using the conventional beamformer, the beam pattern results with amplitude weights determined by the linear minimum variance estimation method were superior to the beam pattern determined by using unity amplitude weights. However in all cases the conventional beamformer was significantly inferior to the beam pattern determined by the linear minimum variance estimation technique in terms of depth resolution.

The linear minimum variance estimation technique could not be used for all ranges with the chosen sound speed profile. For ranges of 187 km and 235 km the relative



travel times produce an 'A' matrix which is so ill-conditioned that the 'IMSL' subroutine 'LINV2F' cannot determine an accurate inverse of 'A<sup>T</sup>A'.

There is sufficient evidence from this initial investigation that the linear minimum variance estimation technique applied to a long linear vertical array can yield high resolution depth information about passive sources at very long ranges. However, further investigation is needed before any field tests are in order. Recommendations for further research are:

1. The use of a more realistic speed of sound profile, preferably one actually characteristic of the 'SCFAR' channel.
2. The use of more hydrophones in the vertical array. As more receivers are used the beam pattern should approach the desired beam pattern more closely (a less overdetermined system should yield smaller total minimum mean square error).
3. Investigation into causes for the peak response falling at other than the desired depth and techniques for correcting this problem when using the linear minimum variance estimation technique.
4. Alternate assumption for choosing the ray paths to include in the 'A' matrix. For example one might choose the rays with the greatest intensity instead of the shortest travel time.
5. The possibility of estimating range as well as the depth of a passive source with linear minimum variance estimation techniques.

In conclusion, the linear minimum variance estimation technique of beamforming was significantly superior to the conventional beamformer. High resolution depth information about passive sources at long ranges is provided.



APPENDIX A  
RELATIVE TRAVEL TIME CALCULATION

This program calculates the relative travel times from each source depth to the horizontal range and the depth of the ray at this range. To save paper, only the two shallowest source depths are listed.

















```

D4=DEPTH
TIME=TIME+(-1.000/G)*DLOG((DTAN(P))/(DTAN(P+(F1/2.000))))
T4=TIME
CDEP=-CDEP*(C1)+1.000
X2=((CDEP*G)/C1)+1.000
F2=CARCCS(X2)
Y2=DSIN(F2)
FRAN=(C1*(-Y2))/G
RAN=RAN+FRAN
R4=RAN
IF (RANGE-RAN)51,51,52
  ADD ARC 6
C1=C1+G*CDEF
DEPTH=DEPTH+CDEP
D5=DEPTH
TIME=TIME+(-1.000/G)*DLOG((DTAN(P+F2/2.000))/(DTAN(P)))
T5=TIME
X1=X2
Y1=Y2
G=0.01700
CDEP=(C1*(1.000-X1))/(G*X1)
GRAN=(C1*Y1)/(G*X1)
RAN=GRAN+RAN
R5=RAN
IF (RANGE-RAN)61,61,62
  ADD ARC 7
C1=C1+G*CDEF
DEPTH=DEPTH+CDEP
D6=DEPTH
TIME=TIME+(-1.000/G)*DLOG((DTAN(P))/(DTAN(P+(F2/2.000))))
T6=TIME
CDEP=-CDEP
X2=(CDEP*G)/C1+1.000
F2=-DARCCS(X2)
Y2=DSIN(F2)
FRAN=(C1*(-Y2))/G
RAN=RAN+FRAN
R6=RAN
IF (RANGE-RAN)71,71,92
  ADD ARC 8
C1=C1+G*CDEF
DEPTH=DEPTH+CDEP

```

C  
C  
52

C  
C  
62

C  
C  
92

THE01450  
THE01460  
THE01470  
THE01480  
THE01490  
THE01500  
THE01510  
THE01520  
THE01530  
THE01540  
THE01550  
THE01560  
THE01570  
THE01580  
THE01590  
THE01600  
THE01610  
THE01620  
THE01630  
THE01640  
THE01650  
THE01660  
THE01670  
THE01680  
THE01690  
THE01700  
THE01710  
THE01720  
THE01730  
THE01740  
THE01750  
THE01760  
THE01770  
THE01780  
THE01790  
THE01800  
THE01810  
THE01820  
THE01830  
THE01840  
THE01850  
THE01860  
THE01870  
THE01880  
THE01890  
THE01900  
THE01910  
THE01920





```

THE01930
THE01940
THE01950
THE01960
THE01970
THE01980
THE01990
THE02000
THE02010
THE02020
THE02030
THE02040
THE02050
THE02060
THE02070
THE02080
THE02090
THE02100
THE02110
THE02120
THE02130
THE02140
THE02150
THE02160
THE02170
THE02180
THE02190
THE02200
THE02210
THE02220
THE02230
THE02240
THE02250
THE02260
THE02270
THE02280
THE02290
THE02300
THE02310
THE02320
THE02330
THE02340
THE02350
THE02360
THE02370
THE02380
THE02390
THE02400

D7=DEPTH
TIME=TIME+(-1.0D0/G)*DLOG((DTAN(P+(F2/2.0D0)))/(DTAN(P)))
T7=TIME
G=-0.017D0
X1=X2
Y1=Y2
CDEP=(C1*(1.0D0-X1))/(G*X1)
RAN1=C1*Y1/(G*X1)
F1=DARSIN(Y1)
RAN=LAN+RAN1
R7=RAN
IF (RANGE-RAN)101,101,102
ADC ARC 9
C
C
C
102
C1=C1+G*CDEF
DEPTH=DEPTH+CDEP
D8=DEPTH
TIME=TIME+(-1.0D0/G)*DLOG((DTAN(P))/(DTAN(P+(F1/2.0D0))))
T8=TIME
CDEP=-CDEP
X2=((CDEP*G)/C1)+1.0D0
F2=DARCCOS(X2)
Y2=DSIN(F2)
RAN2=(C1*(-Y2))/G
RAN=LAN+RAN2
R8=RAN
IF (RANGE-RAN)111,111,112
ADC ARC 10
C
C
C
112
C1=C1+G*CDEF
DEPTH=DEPTH+CDEP
D9=DEPTH
TIME=TIME+(-1.0D0/G)*DLOG((DTAN(P+F2/2.0D0)))/(DTAN(P)))
T9=TIME
X1=X2
Y1=Y2
G=0.017D0
CDEP=(C1*(1.0D0-X1))/(G*X1)
RAN3=(C1*Y1)/(G*X1)
RAN=LAN+RAN3
R9=RAN
IF (RANGE-RAN)121,121,122
ADC ARC 11
C
C
C
122
C1=C1+G*CDEF

```







THE002890  
 THE002900  
 THE002910  
 THE002920  
 THE002930  
 THE002940  
 THE002950  
 THE002960  
 THE002970  
 THE002980  
 THE002990  
 THE003000  
 THE003010  
 THE003020  
 THE003030  
 THE003040  
 THE003050  
 THE003060  
 THE003070  
 THE003080  
 THE003090  
 THE003100  
 THE003110  
 THE003120  
 THE003130  
 THE003140  
 THE003150  
 THE003160  
 THE003170  
 THE003180  
 THE003190  
 THE003200  
 THE003210  
 THE003220  
 THE003230  
 THE003240  
 THE003250  
 THE003260  
 THE003270  
 THE003280  
 THE003290  
 THE003300  
 THE003310  
 THE003320  
 THE003330  
 THE003340  
 THE003350  
 THE003360

SUBROUTINE TO CALCULATE DEPTH AND TIME IF ADDITION OF RANGE OF  
 ARC 2 CAUSES SUMMED RANGE TO BE GREATER THAN SOURCE-RECEIVER  
 RANGE

C  
 C  
 C  
 C  
 21

Y2 = -(RANGE-R11)\*G/C1  
 F2 = DARSIN(Y2)  
 X2 = DCOS(F2)  
 CDEP = C1\*(X2 - 1.000)/G  
 TIME = T2 + (-1.000/G)\*DLOG((DTAN(P+(F2/2.000)))/DTAN(P))  
 DEPTH = C2 + CDEP  
 GO TO 32

USE IF ARC 3 CAUSES OVERFLOW

C  
 C  
 C  
 41

Y2 = Y1 - ((RANGE-R2)\*G\*X1)/C1  
 F2 = DARSIN(Y2)  
 X2 = DCOS(F2)  
 CDEP = C1\*(X2 - X1)/(G\*X1)  
 TIME = T3 + (-1.000/G)\*DLOG((DTAN(P+(F2/2.000)))/DTAN(P+(F1/2.000)))  
 DEPTH = C3 + CDEP  
 GO TO 32

USE IF ARC 4 CAUSES OVERFLOW

C  
 C  
 C  
 51

Y2 = -(RANGE-R3)\*G/C1  
 F2 = DARSIN(Y2)  
 X2 = DCOS(F2)  
 CDEP = C1\*(X2 - 1.000)/G  
 TIME = T4 + (-1.000/G)\*DLOG((DTAN(P+(F2/2.000)))/DTAN(P))  
 DEPTH = D4 + CDEP  
 GO TO 32

USE IF ARC 5 CAUSES OVERFLOW

C  
 C  
 C  
 61

F1 = F2  
 Y2 = Y1 - ((RANGE-R4)\*G\*X1)/C1  
 F2 = DARSIN(Y2)  
 X2 = DCOS(F2)  
 CDEP = C1\*(X2 - X1)/(G\*X1)  
 TIME = T5 + (-1.000/G)\*DLOG((DTAN(P+(F2/2.000)))/DTAN(P+(F1/2.000)))  
 DEPTH = C5 + CDEP  
 GO TO 32

USE IF ARC 6 CAUSES OVERFLOW

C  
 C  
 C  
 71

Y2 = -(RANGE-R5)\*G/C1  
 F2 = DARSIN(Y2)  
 X2 = DCOS(F2)









THE03850  
 THE03860  
 THE03870  
 THE03880  
 THE03890  
 THE03900  
 THE03910  
 THE03920  
 THE03930  
 THE03940  
 THE03950  
 THE03960  
 THE03970  
 THE03980  
 THE03990  
 THE04000  
 THE04010  
 THE04020  
 THE04030  
 THE04040  
 THE04050  
 THE04060  
 THE04070  
 THE04080  
 THE04090  
 THE04100  
 THE04110  
 THE04120  
 THE04130  
 THE04140  
 THE04150  
 THE04160  
 THE04170  
 THE04180  
 THE04190  
 THE04200  
 THE04210  
 THE04220  
 THE04230  
 THE04240  
 THE04250  
 THE04260  
 THE04270  
 THE04280  
 THE04290  
 THE04300  
 THE04310  
 THE04320

```

72 C K=K+1 TIME=RIGHT I
    C Y(K)=DEPTH
    C X(K)=DEPT H
    C WRITE(6,501)X(K),Y(K),DEGRE
    C WRITE(8,501)X(K),Y(K),DEGRE
    C FORMAT(F10.4,F14.7,9X,F12.8)
901 C INCREMENT THE INITIAL DEPRESSION ANGLE BY 0.1 DEGREES AND RESET
    C INITIAL CONDITIONS. REPEAT THE OPERATION R--R RAY
    C INITIAL DEPRESSION ANGLE IS REACHED. LAST RAY FROM SOURCE DEPTH
    C IS AT THIS ANGLE.
    C IF (A1)58,73,73
    C A1=A1+(PI*0.1D0)/180.0D0
73 C RANGE=R
    C DEPTH=C
    C CI=C
    C RANGE=0.0C0
    C TIME=0.0C0
    C Y1=DSIN(A1)
    C X1=DCOS(A1)
    C IF (A1+F3)88,88,57
97 C I=I+1
    C A1=-F3
    C Y1=DSIN(A1)
    C X1=DCOS(A1)
    C IF (I-2)55,55,99
    C THE FOLLOWING SUBROUTINE IS FOR NEGATIVE (UPWARD) INITIAL
    C DEPRESSION ANGLES
96 C A1=ANGLE
98 C RANGE=R
    C DEPTH=C
    C CI=C
    C A1=A1-(PI*0.1D0)/180.0D0
    C Y1=DSIN(A1)
    C X1=DCOS(A1)
    C IF (A1+(-F3))93,53,53
93 C I=I+1
    C A1=F3
    C Y1=DSIN(A1)
    C X1=DCOS(A1)
    C IF (I-4)53,95,99
    C G=-0.017D0
    C R1A=CI*Y1/(C*X1)
53 C

```



THE04330  
 THE04340  
 THE04350  
 THE04360  
 THE04370  
 THE04380  
 THE04390  
 THE04400  
 THE04410  
 THE04420  
 THE04430  
 THE04440  
 THE04450  
 THE04460  
 THE04470  
 THE04480  
 THE04490  
 THE04500  
 THE04510  
 THE04520  
 THE04530  
 THE04540  
 THE04550  
 THE04560  
 THE04570  
 THE04580  
 THE04590  
 THE04600  
 THE04610  
 THE04620  
 THE04630  
 THE04640  
 THE04650  
 THE04660  
 THE04670  
 THE04680  
 THE04690  
 THE04700  
 THE04710  
 THE04720  
 THE04730  
 THE04740  
 THE04750  
 THE04760  
 THE04770  
 THE04780  
 THE04790  
 THE04800

```

82 IF (RANGE-R1)/81,81,82
   CDEP=C1*(1.00-X1)/(G*X1)
   RAN=R1A
   TIME=(-1.00(G/G)*DLOG((DTAN(P))/DTAN(P+(A1/2.000))))
   Y1=1.00C
   Y2=Y1-(RANGE*G*X1)/C1
   F2=DCOS(F2)
   X2=DCOS(X2-X1)/(G*X1)
   TIME=C1*(X2-X1)/(G*X1)
   CDEP=C1*(X2-X1)/(G*X1)
   GO TO 88

81 DEPTH=CDEP+DEPTH
   C1=C1+G*CDEF
   GO TO 88

      K IS THE NUMBER OF RAYS CALCULATED FOR EACH SOURCE DEPTH

CONTINUE
WRITE(6,991)DEPTH,K
WRITE(8,991)DEPTH,K
FORMAT(IX,NUMBER OF RAYS FOR THE ',F7.2,' METER DEPTH IS',IX,13)
WRITE(6,178)
WRITE(8,178)
FORMAT(IX,
      ',1X)

178 CONTINUE
531 INCREMENT THE SOURCE DEPTH 20 METERS UNTIL 600 METERS
C IS EXCEEDED
C
C
C
9 IF (DEPTH-600.000)5,9,9
CONTINUE
STOP
END

DEPTH RELATIVE TRAVEL TIME INITIAL ANGLE
1157.4079 0.0012725 0.0000000
1173.6307 0.0022367 0.0000000
1185.6802 0.0028523 0.0000000
1193.6744 0.0031453 0.0000000
1197.7002 0.0031655 0.0000000
1197.8063 0.0028606 0.0000000
1193.9812 0.0022450 0.0000000
1186.1832 0.0013153 0.0000000
1174.3260 0.0005505 0.0000000
1158.2750 -0.0016306 1.0000000
1137.8606

```



THE04810  
THE04820  
THE04830  
THE04840  
THE04850  
THE04860  
THE04870  
THE04880  
THE04890  
THE04900  
THE04910  
THE04920  
THE04930  
THE04940  
THE04950  
THE04960  
THE04970  
THE04980  
THE04990  
THE05000  
THE05010  
THE05020  
THE05030  
THE05040  
THE05050  
THE05060  
THE05070  
THE05080  
THE05090  
THE05100  
THE05110  
THE05120  
THE05130  
THE05140  
THE05150  
THE05160  
THE05170  
THE05180  
THE05190  
THE05200  
THE05210  
THE05220  
THE05230  
THE05240  
THE05250  
THE05260  
THE05270  
THE05280

NUMBER OF RAYS	FCR TFE	RELATIVE TRAVEL TIME	INITIAL ANGLE	DEPTH
1188	0.037000	0.0184080	0.0000000	142553
1104	0.062330	0.0190509	0.1000000	143234
1106	0.092386	0.0195765	0.2000000	144117
1096	0.128722	0.0199448	0.3000000	144717
913	0.169717	0.0200507	0.4000000	145022
862	0.21090	0.0201025	0.5000000	144783
805	0.255669	0.0199679	0.6000000	144234
753	0.299738	0.0196584	0.7000000	143858
696	0.343231	0.0191709	0.8000000	142385
638	0.386434	0.0184861	0.9000000	140734
580	0.427604	0.0175682	1.0000000	138734
522	0.467510	0.0164489	1.1000000	136690
465	0.504554	0.0150164	1.2000000	134667
409	0.538628	0.0132680	1.3000000	132268
354	0.569386			
302	0.596485			
254	0.620132			
209	0.639836			
165	0.655253			
113	0.667447			
110	0.675970			
81	0.680558			
65	0.683573			
57	0.684673			
47	0.684959			
37	0.685065			
27	0.686560			
18	0.690506			
11	0.699827			
5	0.715197			
1	0.725201			

220.00 METER DEPTH IS 42



THEO5290  
THEO5300  
THEO5310  
THEO5320  
THEO5330  
THEO5340  
THEO5350  
THEO5360  
THEO5370  
THEO5380  
THEO5390  
THEO5400  
THEO5410  
THEO5420  
THEO5430  
THEO5440  
THEO5450  
THEO5460  
THEO5470  
THEO5480  
THEO5490  
THEO5500  
THEO5510  
THEO5520  
THEO5530  
THEO5540  
THEO5550  
THEO5560  
THEO5570  
THEO5580  
THEO5590  
THEO5600

1.40000000  
1.50000000  
1.60000000  
1.70000000  
1.80000000  
1.90000000  
2.00000000  
2.10000000  
2.20000000  
2.30000000  
2.40000000  
2.50000000  
2.60000000  
2.70000000  
2.80000000  
2.90000000  
3.00000000  
3.10000000  
3.20000000  
3.30000000  
3.40000000  
3.50000000  
3.60000000  
3.70000000  
3.80000000  
3.90000000  
4.00000000  
4.10000000  
4.20000000  
4.22688592

240.00 METER DEPTH IS 44

0.0111410  
0.0086388  
0.0055768  
0.00199620  
-0.0023034  
-0.00132848  
-0.00197747  
-0.00260831  
-0.00378035  
-0.00431235  
-0.00523572  
-0.00562538  
-0.00624466  
-0.00667361  
-0.00677407  
-0.00685519  
-0.00692636  
-0.00693339  
-0.00693250  
-0.00694228  
-0.00697576  
-0.00706456  
-0.00721825  
-0.00727444

NUMBER CF RAYS FCR THE

305.5720  
1273.1130  
112382.1432  
111332.7621  
110774.2255  
10032.3854  
8688.1976  
714.7706  
641.7250  
560.9417  
432.0637  
368.6572  
308.4811  
202.9089  
158.6575  
120.9356  
90.1725  
69.3833  
53.3308  
60.7798  
79.5029  
115.2802  
1153.9190  
167.9190





## APPENDIX B

### INTERPOLATION OF RELATIVE TRAVEL TIME CALCULATIONS

This program does an interpolation of the output data generated in Appendix A. The relative travel times are interpolated for the receiving hydrophone depths.











## APPENDIX C

### RESULTING BEAM PATTERN FOR CALCULATED WEIGHTS

This program uses the output of Appendix B to calculate the 'A' matrix. From this, the amplitude and phase weights are determined by the linear minimum variance estimation technique. These weights are applied to the array and the beam pattern is obtained.





```

PROGRAM WHICH DOES THE FOLLOWING TASKS:
* CALCULATES THE 'A' MATRIX FROM RELATIVE TRAVEL TIMES
* CALCULATES ANS WHICH REPRESENTS THE UNKNOWN - THE AMPLITUDE
  AND PHASE WEIGHTS TO BE APPLIED TO THE ARRAY
* USES 'ANS' AND 'A' TO CALCULATE THE RESULTING BEAM PATTERN

DESCRIPTION OF IMPORTANT PARAMETERS

FREQ - FREQUENCY IN HZ
Z - DESIRED BEAM PATTERN (REAL AND IMAGINARY PARTS SEPARATE)
ANS - THE UNKNOWN, PHASE AND AMPLITUDE WEIGHTS DETERMINED BY
      LINEAR MINIMUM VARIANCE METHOD
Y - RESULTING BEAM PATTERN (REAL AND IMAGINARY PARTS SEPARATE)
XX - RESULTING BEAM PATTERN (REAL AND IMAGINARY PARTS COMBINED)
F - RELATIVE TRAVEL TIMES CALCULATED IN APPENDIX B
W - WEIGHTING MATRIX
X1 - SCALFCE DEPTH

      1453P, TIME=56
DIMENSION A(40,10), F(20,5), ANG(20,5), W(40,40), Z(40,1), C(10,40),
*D(10,10), E(10,1), DINV(10,10), WKAREA(150), ANS(10,1),
*B(20,20), Y(40,1), X(20,1), X1(20,1)

SET INITIAL CONDICINS
J1=0
I1=0
I2=0
I19=0
I6=C
I5=0
J5=0
PI=3.14159265358980
FREQ=100.00
P=2.0*PI*FREQ

READ IN THE RELATIVE TRAVEL TIMES DERIVED IN APPENDIX B
READ(5,10)((F(I,J),J=1,5),I=1,20)
FORMAT(5F14.7)

CALCULATE THE 'A' MATRIX.
IF THERE IS NOT A SOUND SIGNAL AT A RECEIVER DEPTH THEN SET THE
SINE AND COSINE TO ZERO.

J1=J1+1

```

```

CCCCCCCCCCCCCCCCCCCC$JOB
CCC
CCC
CCC
10
CCCCC
8

```

```

MA900010
MA900020
MA900030
MA900040
MA900050
MA900060
MA900070
MA900080
MA900090
MA900100
MA900110
MA900120
MA900130
MA900140
MA900150
MA900160
MA900170
MA900180
MA900190
MA900200
MA900210
MA900220
MA900230
MA900240
MA900250
MA900260
MA900270
MA900280
MA900290
MA900300
MA900310
MA900320
MA900330
MA900340
MA900350
MA900360
MA900370
MA900380
MA900390
MA900400
MA900410
MA900420
MA900430
MA900440
MA900450
MA900460
MA900470
MA900480

```



```

7  I1=I1+1, J1=J1, EQ, OIGC TO 6
   IF (F(I1, J1)=P*(I1, J1))
   ANG(I1, J1)=COS(ANG(I1, J1))
   A(I1, J1+5)=SIN(ANG(I1, J1))
   A(I1+20, J1)=-A(I1, J1+5)
   A(I1+20, J1+5)=A(I1, J1)
   IF (I1 - 2C) 7, 2, 2
2  I1=0
   IF (J1 - 5) 8, 72, 72
6  A(I1, J1)=0
   A(I1, J1+5)=C
   A(I1+20, J1)=0
   A(I1+20, J1+5)=0
   IF (I1 - 2C) 7, 2, 2
C  SET WEIGHTING MATRIX TO IDENTITY MATRIX.
C  SET DESIRED BEAM PATTERN 'Z'.
72 I5=I5+1
52 J5=J5+1
   W(I5, J5-4C) 52, 53, 53
53 J5=0
75 IF (I5 - 4C) 72, 75, 75
   I6=I6+1
   Z(I6, I6)=C, 0
   W(I6, I6)=1, C0
76 IF (I6 - 4C) 75, 76, 76
   W(I, I)=1, C0
   Z(I, I)=1, 00
C  THE ENERGY SOURCE IS SELECTED TO BE ON THE SHALLOWEST DEPTH
C  THE IMSL ROUTINE SUMMARY
C  * VMULFF - TRANSPOSE OF FIRST MATRIX TIMES SECOND MATRIX
C  * VMULFF - FIRST MATRIX TIMES SECOND MATRIX
C  * LINV2F - INVERSE OF A MATRIX
C  CONTINUE
CALL VMULFFM(A, W, 40, 10, 40, 40, 40, C, 10, IER1)
CALL VMULFF(C, A, 10, 40, 10, 40, 40, D, 10, IER2)
CALL VMULFF(C, Z, 10, 40, 1, 10, 40, E, 10, IER3)
CALL LINV2F(D, 10, 10, DINV, 3, WKAREA, IER4)
CALL VMULFF(DINV, E, 10, 10, 1, 10, 10, ANS, 10, IER5)
C  PRINT CALCULATED PHASE AND AMPLITUDE WEIGHTS
C

```

```

MA90C490
MA90C500
MA90C510
MA90C520
MA90C530
MA90C540
MA90C550
MA90C560
MA90C570
MA90C580
MA90C590
MA90C600
MA90C610
MA90C620
MA90C630
MA90C640
MA90C650
MA90C660
MA90C670
MA90C680
MA90C690
MA90C700
MA90C710
MA90C720
MA90C730
MA90C740
MA90C750
MA90C760
MA90C770
MA90C780
MA90C790
MA90C800
MA90C810
MA90C820
MA90C830
MA90C840
MA90C850
MA90C860
MA90C870
MA90C880
MA90C890
MA90C900
MA90C910
MA90C920
MA90C930
MA90C940
MA90C950
MA90C960

```



```

999 WRITE(6,999)
      FORMAT(IX,ANS MATRIX (PHASE AND AMPLITUDE WEIGHTS) FOLLOWS.)
158 WRITE(6,158)(ANS(I8,1),I8=1,10)
      FORMAT(F14.7)
C
C   APPLYING THESE PHASE AND AMPLITUDE WEIGHTS, THE RESULTING BEAM
C   PATTERN IS CALCULATED (REAL AND IMAGINARY PARTS SEPARATE)
760 CALL VMLFF(A,ANS, 40,10,1,40,10,Y,40,IER2)
C
C   THE REAL AND IMAGINARY PARTS OF THE RESULTING BEAM PATTERN
C   ARE COMBINED TO GIVE ABSOLUTE VALUE.
987 I20=I20+1
      XX(I20,1)=SQRT(Y(I20,1)*Y(I20+20,1)+Y(I20+20,1)*Y(I20+20,1))
      IF(I20-20)987,654,654
      I19=I19+1
      XI(I19,1)=2(0.0+I19*20.0
      IF(I19-20)654,655,655
C
C   PRINT SOURCE DEPTH AND ABSOLUTE VALUE OF BEAM PATTERN AT
C   THAT DEPTH
C
C   WRITE(6,588)(X1(I,1),XX(I,1),I=1,20)
655 WRITE(9,588)(X1(I,1),XX(I,1),I=1,20)
988 FORMAT(FE.2,' METER DEPTH' HAS STRENGTH CF ',F14.7)
172 CONTINUE
      STOP
      END
$ENTRY
ANS MATRIX (PHASE AND AMPLITUDE WEIGHTS) FOLLOWS
-0.0050524
-2.275893C
-0.5812412
-4.330297C
-0.2429767
-1.373913C
-3.074544C
-2.144663C
C.712266E1

```

```

MA90C570
MA900580
MA900590
MA901000
MA901010
MA901020
MA901030
MA901040
MA901050
MA901060
MA901070
MA901080
MA901090
MA901100
MA901110
MA901120
MA901130
MA901140
MA901150
MA901160
MA901170
MA901180
MA901190
MA901200
MA901210
MA901220
MA901230
MA901240
MA901250
MA901260
MA901270
MA901280
MA901290
MA901300
MA901310
MA901320
MA901330
MA901340
MA901350
MA901360
MA901370
MA901380
MA901390
MA901400
MA901410
MA901420
MA901430
MA901440

```









## LIST OF REFERENCES

1. Officer, C. E., Introduction to the Theory of Sound Transmission, McGraw-Hill, 1958.
2. Kinsler, L. E., and others, Fundamentals of Acoustics, Wiley, 1982.
3. Melsa, J. L. and Cohn, A. B., Decision and Estimation Theory, McGraw-Hill, 1978.



## INITIAL DISTRIBUTION LIST

		No. Copies
1.	Defense Technical Information Center Cameron Station Alexandria, Virginia 22314	2
2.	Library, Code 0142 Naval Postgraduate School Monterey, California 93943	2
3.	Department Chairman, Code 62 Department of Electrical Engineering Naval Postgraduate School Monterey, California 93943	1
4.	Professor P.H. Mose, Code 62Me Department of Electrical Engineering Naval Postgraduate School Monterey, California 93943	6
5.	Professor L.J. Ziomek, Code 62Zm Department of Electrical Engineering Naval Postgraduate School Monterey, California 93943	1
6.	Lt (N) D.P. McVicar 33 Hawthorne St. Antigonish, Nova Scotia B2G 1A2 Canada	4
7.	EMCS-3 National Defence Headquarters Ottawa, Ontario K1A 0K2 Canada	4
8.	DPED National Defence Headquarters Ottawa, Ontario K1A 0K2 Canada	2
9.	Captain D. Cantley 4073 El Bosque Febble Beach, California 93953	1













297507

Thesis

M272 McVicar

c.1 Amplitude shading  
and phase weighting of  
a vertical linear array  
in the SOFAR channel by  
the linear minimum var-  
iance estimation tech-  
nique.

297507

Thesis

M272 McVicar

c.1 Amplitude shading  
and phase weighting of  
a vertical linear array  
in the SOFAR channel by  
the linear minimum var-  
iance estimation tech-  
nique.



thesM272

Amplitude shading and phase weighting of



3 2768 002 03372 2

DUDLEY KNOX LIBRARY